Title
THE EFFECT OF A LONG RANGE INTERATOMIC POTENTIAL ON THE STABILITY OF CRYSTAL LATTICES

Author
Krause, Charles William.

Publication Date
1974-09-01

LBL-3151

THE EFFECT OF A LONG RANGE INTERATOMIC POTENTIAL ON THE STABILITY OF CRYSTAL LATTICES

Charles William Krause
(Ph. D. thesis)

September 1974

Prepared for the U. S. Atomic Energy Commission
under Contract W-7405-ENG-48

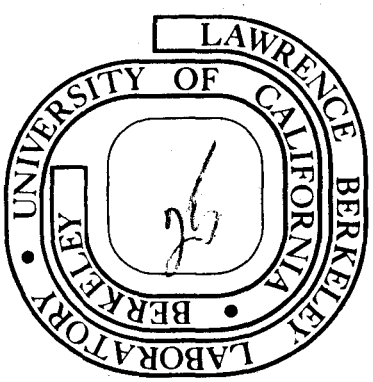

LBL-3151

DISCLAIMER

Consult yourself, and if you find
A powerful Impulse urge your Mind,
Impartial judge within your Breast
What Subject you can manage best;
Whether your Genius most inclines
To Satire, Praise, or hum'rous Lines;
To Elegies in mournful Tone,
Or Prologue sent from Hand unknown.
Then rising with Aurora's Light,
The Muse invok'd, sit down to write;
Blot out, correct, insert, refine,
Enlarge, diminish, interline;
Be mindful, when Invention fails,
To scratch your Head, and bite your Nails.

from On Poetry: A Rapsody

by *Jonathan Swift, 1733*

THE EFFECT OF A LONG RANGE INTERATOMIC POTENTIAL ON THE STABILITY OF CRYSTAL LATTICES

Table of Contents

THE EFFECT OF A LONG RANGE INTERATOMIC POTENTIAL ON THE STABILITY OF CRYSTAL LATTICES

Charles William Krause

Inorganic Materials Research Division, Lawrence Berkeley Laboratory and Department of Materials Science and Engineering, College of Engineering; University of California, Berkeley, California

ABSTRACT

The mechanical and phase stability of metallic crystal lattices is studied with a long range interatomic potential which describes the bonding between atoms in the lattice. Particular attention is accorded to phenomena related to the shear of close-packed planes across one another in close-packed polytypes.

The long range potential, which oscillates with increasing interatomic separation, can be partially summed to obtain an interplanar interaction which is particularly useful for the study of shear phenomena. Use of the interatomic potential, referred to as the Friedel potential, and the interplanar interaction allow the calculation of the relative energies of competing lattice structures, of phonon dispersion relations, elastic constants, stacking fault energies and the determination of the effects of finite homogeneous deformations of simple metallic crystals. The various phenomena and structures are studied at constant volume and as a function of the valence of metallic alloy.

I. INTRODUCTION

Although theories of metallic bonding presently have limited usefulness, some properties of metallic elements and alloys cannot be understood without an understanding of phenomena occurring in regions of atomic dimension. For example, the strong dependence of properties on trace impurities or the effects of interstitial atoms and vacancies on the properties of materials subjected to irradiation will probably not yield easily to empirical analysis alone. Approaches to the determination of how atoms within a metal are bonded together on a microscopic scale are needed to unravel these and other effects. One such approach is the pseudopotential theory[1] of metallic bonding which will be used in the study of the stability of metallic crystal lattices found below. While such a study may not allow the immediate attainment of desirable metallurgical properties from an alloy, it is through such studies that systematic control of properties can emerge.

The pseudopotential theory of metallic bonding itself provides a relatively simple method for computing the energies of a variety of structures into which atoms can arrange themselves in metals. The energies associated with different crystal structures, dislocations, stacking faults, ordering phenomena, etc., can all be calculated using pseudopotential theory. While the accuracy of the energies so obtained varies according to the particular structure being investigated, the method is of general applicability. In this regard, pseudopotential theory is to metals what molecular orbital theory is to organic chemistry--a branch of applied quantum mechanics with a broad range of

applicability made possible by the use of approximations which have proved to be fairly good in practice. Molecular orbital theory is easier to use than pseudopotential theory; however, pseudopotential theory must account for energies an order of magnitude smaller than those usually required by the users of molecular orbital theory.

One of the problems found in the application of pseudopotential theory is that in its more usual form, the theory is cast in the language of reciprocal space and not directly in terms of real space parameters. From the metallurgist's point of view, a real space theory is preferable to a reciprocal space theory of bonding for two reasons. First, a real space formulation is more easily visualized than a reciprocal space version of a bonding theory. Secondly, any relaxation process, whereby the positions of the atoms (or more precisely, ions) are iterated to find the low energy configurations of defected crystals, can be treated more directly in real space. These advantages are present in the real space formulation of the pseudopotential theory of metallic bonding as formulated by Cohen[2] and Harrison.[1] In fact, the application of second order perturbation theory to the interaction between the electron gas and the ionic pseudopotentials leads to the expression of ε, the structure dependent energy per ion (at constant atomic volume), as the sum of a central interionic potential over pairs of ions in the metallic crystal:

$$\varepsilon = \frac{1}{2N} \sum_{i \neq j} V(r_{ij}) , \qquad (I.1)$$

where V(r) is the interionic potential, r_{ij} is the distance separating the $i^{\underline{th}}$ and $j^{\underline{th}}$ ions, and N is the number of ions in the crystal. The evaluation of Eq. (I.1) provides the basis for the conceptually simple calculations found below.

A number of different interionic potentials could be used in Eq. (I.1). For example, if the electron gas were not present, and the ions were well separated, the appropriate form for the potential would be

$$V(r) = \frac{Z^2 e^2}{r} \tag{I.2}$$

where Z is the valence of the ions. With Eq. (I.2) in Eq. (I.1), the average electrostatic energy per ion of the array of positive ions is obtained. When the electron gas is present, the interionic potential is weakened and behaves like

$$V(r) = V_o \frac{\cos 2k_F r}{(2k_F r)^3} \tag{I.3}$$

for large r, where k_F is the Fermi wave-vector and V_o is a constant which is independent of structure. The electrons neutralize in a sense, or screen, the electrostatic interaction, Eq. (I.2), and Eq. (I.3) is the form of the residual interaction. The Fermi wave-vector is just

$$k_F = 2\pi/\lambda_F$$

long-ranged function, and below, some of the consequences of the range of the Friedel potential will emerge. However, interatomic potentials other than the Friedel potential can give similar results, so that conclusive statements about the range of interaction will be difficult to make. The second question deals with phase transformations and specifically the connection between the two or more structures involved in any phase transformation. In particular, it is desired to know if there are manifestations of a phase transformation in the microscopic parameters characterizing the phases, and, if so, do they give information about the manner in which the transformation proceeds. Since neither pressure nor temperature enter the analysis below, no transformations can be studied directly. However, much of what is done below is an attempt to understand the mechanisms of structural phase transformations.

As mentioned above, one of the best features of pseudopotential theory is that it provides a relatively simple, versatile method for studying many phenomena. In order to maintain this simplicity and versatility while using the real space formulation of pseudopotential theory to study structural stability, a particular technique will be emphasized whereby partial sums of the Friedel potential over planes of atoms are performed to obtain the interaction between planes. A very simple interplanar interaction arises and allows the calculation of stacking fault energies, twin boundary energies, relative energies of polytypes, elastic constants, phonon dispersion relations, etc. In fact, experimental work on lattice vibrations is sometimes interpreted with the aid of interplanar force constants.[5] Use of what will be

termed the interplanar interaction was first made by Blandin, Friedel and Saada[6] and gives rise to particularly simple algebraic forms and very easy ways of visualizing the various aspects of the study of structural stability below.

A complete study of the stability of lattices of ions interacting according to the Friedel potential would be an arduous task; no such thing appears below. Instead, we have concentrated on the aspects of stability associated with simple polytypic structures, such as the face-centered cubic and hexagonal close-packed structures, and the various phenomena associated with the shear of the close-packed planes across one another. Other topics appear, but the main thrust is towards understanding close-packed polytypes and displacements perpendicular to the stacking direction in these polytypes.

In the next chapter, some of the theoretical background material requisite for the subsequent use of the real space formulation of pseudopotential theory is developed. Chapter III concerns the evaluation of the sums that arise in later chapters. The method for the evaluation of Eq. (I.1) using the Friedel potential for three dimensional lattices is discussed along with a derivation of the interplanar interaction and an interlinear interaction. The latter is the result of another partial sum and is not used in any subsequent calculation, but is included to complete the development of the sums of the Friedel potential over crystal lattices. The contents of Chapter IV are concerned with the use of the Friedel potential for the study of stability of lattices against phase transformation, i.e., the determination of the structure

with the minimum energy at T=0K from among a selected set of simple structures. Some of this material has already been published separately.[7] Chapter V includes the calculation of phonon dispersion relations and elastic constants using the interplanar interaction. The treatment is probably too abbreviated to do justice to this broad topic. However, measurements of the Debye-Waller factor, elastic constants, phonon dispersion curves, etc., all indicate that much is to be learned about phase transformations through the study of various modes of softening of crystal lattices. Phase transformations, of course, are of great practical importance, and whatever can be said about the instabilities which give rise to phase transformations is of some use. Chapter VI concerns the further aspects of the study of lattice stability which are of importance, but which have not yet been investigated in great detail. First, the method of Blandin et al.[6] for the determination of stacking fault and twin energies is discussed. Then finite homogeneous deformations are treated, albeit somewhat briefly, since this subject is intimately related to the study of elastic constants, mechanical stability and stability against phase transformations. The concluding chapter compares the different criteria for stability which emerge in the preceding chapters and indicates to what extent the Friedel potential might accurately predict physical phenomena. Throughout, emphasis will be placed on the interpretation of various phenomena and their interrelationships rather than numerical results.

II. THEORETICAL BACKGROUND

The pseudopotential theory of simple metals has yielded several models which promise to be useful in the prediction of structure.[1,8] The simplest and most general of these follows from Harrison's[1] development of Cohen's[2] real space formulation of the pseudopotential theory. If a pseudopotential model of a simple metal is developed to second order in perturbation theory, that part of the cohesive energy which depends on the structure may be treated as if the atoms interacted in pairs according to a central, two-body potential. This two-body potential has an asymptotic form which is independent of the precise pseudopotential assumed, and which exhibits the Friedel[4] oscillations. Under suitable assumptions, discussed below, one may make a rough estimate of the relative energies of candidate structures at 0 K by simply summing the energy of two-atom interactions according to the asymptotic, or Friedel potential. This approach has been taken in several studies of the structure of simple metals and alloys[6,9-11] and is followed below, where we supplement prior work with new computations to explore the results of a simple structural model based on the two-body Friedel potential.

While the approximations involved in a structural model based on the Friedel potential are drastic, the model has several attractive features. It leads to equations which are easy to use and which incorporate aspects of the more fundamental theory while avoiding the recalcitrant problem of choosing proper pseudopotentials. Moreover,

the model yields a prediction of alloy structure which is based on the electron-atom ratio, in the spirit of the Hume-Rothery[12] and Engel-Brewer[13] correlations, and which is in general agreement with known structural tendencies in simple metals and alloys.

The central equations of the structural model used here are derived as follows. Employing the real space formulation of the pseudopotential theory of a simple metal[1] the cohesive energy per atom may be developed in the perturbation series:

$$E = E_o + E_1 + E_2 + \ldots \qquad \text{(II.1)}$$

whose successive terms involve perturbations of increasing order. The zeroth and first order terms in this expansion depend on the volume per atom (Ω), but are independent of structure. The second order term, E_2, is the first to show the influence of structure. It can be cast in the form

$$E_2 = \frac{1}{2N} \sum_{i,j}{}' V(r_{ij}) \qquad \text{(II.2)}$$

where N is the number of atoms, r_{ij} is the distance between the $i^{\underline{th}}$ and $j^{\underline{th}}$ atom cores, and the prime on the summation indicates that terms having i=j are to be omitted. The function $V(r_{ij})$ appearing in the summation acts as a two-body potential in a restricted sense: it governs the change of energy in a relative displacement of atoms i and j which leaves the atomic volume, and hence E_o and E_1, constant.

If we fix the atomic volume and neglect higher order terms in the perturbation expansion,[1] the relative energy of a given structure is measured by E_2; that structure which minimizes E_2 will be preferred at 0 K.

Computation of the structural energy, E_2, requires a specific expression for the effective interatomic potential, V(r). This potential is sensitive to the details of the pseudopotential used.[1,8] However, irrespective of the pseudopotential, V(r) has the asymptotic form[1]

$$V(r) = V_o \frac{\cos 2k_F r}{(2k_F r)^3} \tag{II.3}$$

when $(k_F r)$ is large, where k_F is the Fermi wave number. In general, V_o depends on the parameters of the pseudopotential in a rather complicated way, but for the case of a local pseudopotential, one which is strictly a multiplicative operator, the form is simple:

$$V_o = \frac{9\pi Z^2 w_{2k_F}^2}{E_F} \tag{II.4}$$

where w_{2k_F} is the value of the screened pseudopotential at $k=2k_F$. It is usually the screened pseudopotentials that are tabulated; Table I lists some typical values of V_o.

We may hence define a dimensionless two-body potential

$$v(r) = \frac{V(r)}{V_o} \tag{II.5}$$

which becomes the Friedel potential

$$v(r) = \frac{\cos 2k_F r}{(2k_F r)^3} \qquad \text{(II.6)}$$

when $k_F r$ is large. If we now uniformly approximate V(r) by its asymptotic form, the structural energy, E_2, may be rewritten in a dimensionless form which is independent of the pseudopotential:

$$\varepsilon = \frac{E_2}{V_o} = \frac{1}{2N} \sum_{i,j}{}' \cos(2k_F r_{ij})/(2k_F r_{ij})^3 \qquad \text{(II.7)}$$

In fact, the dimensionless energy, $\varepsilon=\varepsilon(Z)$, is a function of structure and electron-atom ratio (Z) only; since the separation distances (r_{ij}) in a given structure scale as $\Omega^{1/3}$, where Ω is atomic volume, and since the Fermi wave number, k_F, is $k_F=(3\pi^2 Z/\Omega)^{1/3}$, the set of values of the quantity ($k_F r_{ij}$) in a given structure, and hence the dimensionless energy of the structure, is determined by Z.

Equation (II.7) was drawn from the pseudopotential theory of simple metals. It may be generalized to estimate the relative energies of the structures of uniform random solid solutions of simple metals through use of the virtual crystal model:[8] the alloy is represented as a one-component simple metal made up of pseudoatoms whose properties average those of the atoms actually present. With this approximation the dimensionless structural energy of the solid solution is determined by its mean electron-atom ratio (Z) through Eq. (II.7). The preferred structure of the solid solution at 0 K may then be estimated by

minimizing ε over the set of candidate structures. The result is uniquely determined by Z. For ordered structures, the sum, Eq. (II.2) cannot be so simply separated.

The structural model developed above depends on three specific assumptions, which we discuss in turn.

(1) The effective interatomic potential obtained from the second order pseudopotential theory is replaced by its asymptotic form, the Friedel potential. While it has been found[1] that the effective interatomic potential actually converges toward the Friedel potential rather quickly, important contributions to the structural energy due to near-neighbor interactions may be misestimated. The model is most reasonable when applied to close-packed structures having ideal axial ratios since these differ from one another only in the third (or higher) coordination shells. The model may not yield good values for the relative energies of structures such as fcc and bcc, which differ in the first coordination shell. As we shall show, however, it does provide an empirically reasonable estimate of the range of Z values over which the bcc structure is preferred to the close-packed structures.

(2) The variation in equilibrium atomic volume between candidate structures is ignored. Since small volume changes are observed in solid state transformations, and since these changes (at least at 0 K) must minimize the total energy of the structure, their neglect will necessarily result in an overestimate of the energy advantage enjoyed by the preferred structure. On the other hand, since the atomic volume is left unknown in the calculation of structural energy, this approximation

cannot cause an erroneous identification of the preferred structure.

(3) Alloy solid solutions are treated as if they were composed of identical pseudoatoms having average properties. While the approximations involved in this virtual crystal model are known[8] their quantitative consequences are not. The factors neglected include the tendency to short-range order, the contribution to cohesion from charge transfer between different species, the decrement to cohesion due to local lattice strain caused by size difference between species, and possible error from the second order theory if the valences of the species differ. Of course, these factors are relevant only insofar as they influence the relative energies of candidate structures. The probable error should become more important as size or valence differences become greater.

As noted above, the approach to crystal structure employed here has been used by a number of previous workers. Shaw[9] applied a method due to Epstein[14] to show how Eq. (II.7) may be conveniently set up for direct numerical solution for an arbitrary lattice and computed structural energies for the face-centered cubic (fcc), hexagonal close-packed (hcp) and body-centered cubic (bcc) structures as functions of valence. In related work, Blandin, Friedel and Saada[6] showed that when a structure is close-packed, Eq. (II.7) may be recast in the form of a potential approximating the interaction between close-packed planes. Blandin, Friedel and Saada determined the energies of stacking faults in the fcc and hcp structures and found the ranges of valence over which these structures should be stable with respect to faulting.

Recently, Hodges[10] suggested that the interplanar interaction might be used to simplify Eq. (II.7) for an arbitrary close-packed structure. He employed this formulation in a semiquantitative discussion of the stability of the close-packed polytypic structures occasionally observed in alloy systems. Havinga, van Vucht and Buschow[11] have also discussed phase stability using interplanar interactions of a similar form. Cousins[15] has discussed elastic constants using Shaw's method for the evaluation of Eq. (II.7). These results are summarized and supplemented in the following sections.

III. LATTICE SUMS

While the expressions for the structure-dependent energy of a metallic crystal which were presented in Chapter II provide the basis for the determination of many properties of simple metals, the evaluation of the sums involved can become rather difficult. First, the sums, especially in the real space formulation, e.g., Eq. (II.7), do not converge as rapidly as might be desired and care must be taken to ensure proper accuracy during their evaluation. Secondly, the determination of the configuration of all of the ions in the crystal is required for the evaluation of the sum in Eq. (II.7), and when complicated defects such as dislocations are present, the problem can become immense. In particular, if it is desired to relax the configuration of ions to obtain a minimum energy configuration, then the positions of the ions must be changed in some iterative procedure, and the evaluation of the sums must be repeated until the minimum energy configuration is found. Methods for evaluation of sums such as Eq. (II.7) which are fast and accurate are desired. The purpose of this chapter is to evaluate sums and partial sums of Eq. (II.7) in order to obtain expressions that will provide such methods for both perfect and defected lattices.

The present chapter is divided into three sections. In the first section, the interaction of an ion at a lattice site with the rest of the ions in the metal will be determined by summing the Friedel potential over a regular three dimensional lattice of ions. The method and

formulae are taken directly from Shaw,[9] except for corrections of misprints in his equations and slight modifications of the definitions of dimensionless parameters. These sums will be used later to discuss phase stability. In the second section, the partial sum for an ion interacting with a regular planar lattice is considered. The technique is originally due to Blandin, Friedel and Saada[6] and allows a useful decomposition of the sum in Eq. (II.2). The third section will concern itself with the interaction of an ion with a linear array of ions. Again, a useful decomposition of Eq. (II.2) occurs. The technique is suggested by the work of Blandin et al. and was first developed by Rabier and Grilhe.[16] As might be surmised, the interlinear interaction proves to be most useful in the study of linear defects, i.e., dislocations. The advantage of using the interplanar and interlinear interactions is that once they have been derived, the evaluation of the sum for the total energy consists of sums of the interactions between pairs of planes or lines of atoms. These sums are relatively easy to evaluate and their physical significance is easy to visualize.

A. Exact Summation Method

If the ions of a metal are in crystallographically equivalent positions, as they are in fcc, hcp and bcc lattices, the expression for ε given by Eq. (II.7) can be simplified. For N sufficiently large so that the atoms near the surface of the crystal make a negligible

contribution, one of the sums in Eq. (II.7) can be performed to obtain

$$\varepsilon = \frac{1}{2} \sum_i{}' \frac{\cos 2k_F r_i}{(2k_F r_i)^3} \qquad \text{(III.1)}$$

where r_i is the distance between the $i^{\underline{th}}$ ion and a reference ion.

Shaw[9] developed the summation method of Epstein[14] for the exact summation of Eq. (III.1) for lattices with or without bases. Epstein's method is a general technique for summing quantities like $\exp(ikr)/r^n$ over collections of lattice points and provides the bases for Madelung and Ewald-Fuchs summations. The method involves a transformation of the sum into two rapidly converging sums. The sum over lattice points in real space remains, but an exponential damping factor, which converges to zero rapidly as r_i increases, appears in each term. The residue of the original sum is Fourier transformed into a sum in reciprocal space; each term in this sum includes a damping factor also. An adjustable parameter allows the rate of convergence of the two sums to be adjusted until both converge with equal rapidity, allowing a minimum number of terms to be included in the sums.

Upon transformation, Eq. (III.1) becomes

$$\varepsilon = \frac{1}{2}\sum_{i}{}' \frac{\cos(kr_i)}{(kr_i)^3} = \frac{\pi}{2\Omega}\sum_{q}{}' \frac{|S(q)|^2}{k^3}\left[\left(1+\frac{k}{q}\right)E_1(\alpha) + \left(1-\frac{k}{q}\right)E_1(\beta)\right] \qquad \text{(III.2)}$$

$$+ \frac{4\pi}{\Omega k^3}\left[E_1(k^2/4\omega) - 2e^{-k^2/4\omega}\right] + \frac{1}{2}\sum_{i}{}' \frac{\cos(kr_i)}{(kr_i)^3}\left[\operatorname{erfc}(\omega^{1/2}r_i) + 2\left(\frac{\omega r_i^2}{\pi}\right)^{1/2} e^{-\omega r_i^2}\right] - \frac{2}{3k^3}\left(\frac{\omega^3}{\pi}\right)^{1/2}$$

where

$$k = 2k_F ,$$

$$\alpha = (k+q)^2/4\omega ,$$

$$\beta = (k-q)^2/4\omega ,$$

$$E_1(x) = \int_x^\infty dt \{\exp(-t)/t\} ,$$

$$\mathrm{erfc}(x) = 1 - \mathrm{erf}(x) = 1 - \frac{2}{\sqrt{\pi}} \int_0^x dt \exp(-t^2) ,$$

i labels the lattice points, ω is the convergence parameter, Ω is the atomic volume, and

$$S(q) = \frac{1}{N} \sum_i \exp - i\vec{q}\cdot\vec{r}_i \qquad \text{(III.3)}$$

is the structure factor for the lattice in question. The inclusion of the structure factor in Eq. (III.2) by Shaw allows the sum to be performed for Bravais lattices which have a basis, e.g., the hexagonal close-packed lattice. Also desired is an expression for the sum of $\sin 2k_F r/(2k_F r)^3$ over the lattice:

$$\frac{1}{2}{\sum_i}' \frac{\sin 2k_F r_i}{(2k_F r_i)^3} =$$

$$\frac{\pi^2}{\Omega}{\sum_q}' \frac{|S(q)|^2}{k^3 q} [(\omega\alpha)^{1/2} \mathrm{erfc}(\alpha^{1/2}) - (\omega\beta)^{1/2} \mathrm{erfc}(\beta^{1/2}) - (\frac{\omega}{\pi})^{1/2} (e^{-\alpha} - e^{-\beta})]$$

$$+ \frac{1}{2}{\sum_i}' \frac{\sin kr_i}{(kr_i)^3} \exp -\omega r_i^2 + \frac{\pi^2}{\Omega k^3} \mathrm{erfc}(k/2\omega^{1/2}) - \frac{\omega}{2k^2} \qquad \text{(III.4)}$$

with the same notation as in Eq. (III.2).

As noted in Chapter II, Eq. (III.2) yields a dimensionless energy which depends only on the valence, Z. It is desired that this fact be reflected in the performance of the sum. By casting the parameters appearing in Eqs. (III.2) and (III.4) in dimensionless form, this can be accomplished. Another advantage of doing this is the ease with which the sums can be computed in their new form. By letting $\Omega=r_o^3$ and defining

$$\begin{aligned} R &= \left(\frac{r_o}{2\pi}\right) q & q &= \frac{2\pi}{r_o} R \\ Q &= \left(\frac{r_o}{2\pi}\right) k & k &= \frac{2\pi}{r_o} Q \\ W &= \omega r_o^2 & \omega &= \frac{W}{r_o^2} \\ D_i &= \frac{r_i}{r_o} & r_i &= r_o D_i \end{aligned} \qquad \text{(III.5)}$$

equations (III.2) and (III.4) become

$$\frac{1}{2}\sum_{r_i}{}' \frac{\cos kr_i}{(kr_i)^3} = \frac{\pi}{2(2\pi Q)^3} \sum_{R}{}' |S(R)|^2 \left[\left(1+\frac{Q}{R}\right)E_1(\alpha) + \left(1-\frac{Q}{R}\right)E_1(\beta)\right]$$

$$+ \frac{1}{2}\sum_{D_i}{}' \frac{\cos 2\pi Q D_i}{(2\pi Q D_i)^3} \left[\operatorname{erfc}(\omega^{1/2} D_i) + 2\left(\frac{WD_i^2}{\pi}\right)^{1/2} \exp -WD_i^2\right]$$

$$+ \frac{4\pi}{(2\pi Q)^3}\left[E_1((2\pi Q)^2/4W) - 2\exp -(2\pi Q)^2/4W\right] - \frac{2}{3(2\pi Q)^3}\left(\frac{W^3}{\pi}\right)^{1/2} \qquad \text{(III.6)}$$

and

$$\frac{1}{2}\sum_{r_i}{}' \frac{\sin kr_i}{(kr_i)^3} = \pi^2 W^{1/2} \sum_{R}{}' \frac{|S(R)|^2}{(2\pi)^4 Q^3 R} \cdot$$

$$[\alpha^{1/2}\ \mathrm{erfc}\ \alpha^{1/2} - \beta^{1/2}\ \mathrm{erfc}\ \beta^{1/2} - \pi^{-1/2}\ e^{-\alpha} + \pi^{-1/2}\ e^{-\beta}]$$

$$+ \frac{1}{2}\sum_{D_i}{}' \frac{\sin 2\pi Q D_i}{(2\pi Q D_i)^3}\ \exp -W D_i^2 + \frac{\pi^2}{(2\pi Q)^3}\ \mathrm{erfc}(\pi Q/W^{1/2}) - \frac{W}{2(2\pi Q)^2} \cdot \qquad \text{(III.7)}$$

Equations (III.6) and (III.7) will be used later to discuss the stability of simple structures as a function of Z as well as to determine the stability of these structures against simple deformations away from the structures.

B. The Interplanar Interaction

The formulae presented in the previous section for sums of the Friedel potential over a three-dimensional lattice of ions are ponderous, and simplification of the sums would be desireable. This simplification can often be accomplished by the use of the partial sums derived in this section and the next. In this section, the interaction of an ion with a regular planar lattice of ions is obtained by summing the Friedel potential over the planar lattice. If the ion in question belongs to a plane which is parallel to and has the same symmetry and translation vectors as the original plane, then it is a trivial task to sum to obtain the interaction of the two planes, i.e.,

an interplanar interaction. The technique is originally due to Blandin, Friedel and Saada[6] who used the interplanar interaction to discuss faulting in simple metals with the asymptotic form of the interplanar interaction, which will also be derived below.

Two generalizations of the results of Blandin et al. will emerge below. The interplanar interaction will be cast in a form in which the c/a ratio enters as an explicit variable. This development allows the interplanar interaction to be used for rhombohedral modifications of cubic lattices and for hcp lattices with non-ideal axial ratios (i.e., hcp lattices with $c/a \neq 1.633$). The second generalization is in some sense trivial and is simply the generalization of the interplanar interaction to lattices which contain more than one atom for each site of the hexagonal planar lattice. Laves phases and tetrahedrally bonded valence compounds are among the structures which have this geometry. The introduction of two or more elemental species will not allow the structure to be determined by Z alone, as is the case for solid solutions and elements. However, a useful form results from the relatively simple transformations that yield the generalization of the interplanar interaction.

To obtain the interplanar interaction, consider an ion at a distance z from a plane of ions, and let $\vec{b}$ designate the displacement from the projection of the ion to one of the ions lying in the plane (Fig. 1). Let $\vec{\rho}_i$ designate the positions of the ions in the plane with respect to the ion at $\vec{z}+\vec{b}$. Thus $\vec{z}$ is perpendicular to the plane of ions, while $\vec{b}$ and $\vec{\rho}_i$ lie in the plane of ions. By summing over $\vec{\rho}_i$,

the interaction of the ion with the plane of ions is obtained. This quantity is designated $\phi(z)$:

$$\phi(z) = \sum_i v(|\vec{z} + \vec{b} + \vec{\rho}_i|) \tag{III.8}$$

where

$$v(r) = \frac{\cos 2k_F r}{(2k_F r)^3}$$

is the Friedel potential and k_F is the Fermi wave vector.

The quantity $\phi(z)$ can be expressed in a form in which the sum over i in Eq. (III.8) is replaced by a sum over reciprocal lattice vectors of a planar lattice. This new form is obtained by the introduction of the structure factor of the planar lattice of ions and has the merit that it converges more rapidly than the real space sum. Letting the Friedel potential be the Fourier transform of w(k) (See Appendix A for a derivation of w(k)), we have

$$v(r) = \frac{2\Omega}{(2\pi)^3} \int d^3k\, w(k) \exp - i\vec{k}\cdot\vec{r} \tag{III.9}$$

where Ω is the atomic volume. Noting that $\vec{k}$ can be decomposed into components parallel and perpendicular to $\hat{z}$, denoted $\vec{k}_\parallel$ and $\vec{k}_\perp$, Eq. (III.9) can be rewritten as

$$\phi(z) = \frac{2\Omega}{(2\pi)^3} \sum_i \int d^3k\, w(k)\, \exp -ik_\parallel z\, \exp -i\vec{k}_\perp \cdot (\vec{\rho}_i + \vec{b}) \tag{III.10}$$

Now the structure factor for a planar lattice is just

$$\frac{1}{N} \sum_i \exp - i\vec{k}_\perp \cdot \vec{\rho}_i = \frac{(2\pi)^2}{NA} \sum_{g_\perp} \delta(\vec{k}_\perp - \vec{g}_\perp) \qquad \text{(III.11)}$$

where N is the number of ions in the plane, A is the area of a unit cell of the planar lattice and $\vec{g}_\perp$ denotes the reciprocal lattice vectors of the planar lattice (See Appendix C). Use of (III.11) in (III.10) yields

$$\phi(z) = \sum_{g_\perp} \exp - i\vec{g}_\perp \cdot \vec{b} \left(\frac{2\Omega}{2\pi A} \int_{-\infty}^{\infty} dk_\parallel \exp - ik_\parallel z \; w\left(\sqrt{k_\parallel^2 + g_\perp^2}\right)\right) \qquad \text{(III.12)}$$

Setting the quantity in parentheses equal to $\psi(g_\perp, z)$ and noting that if $\vec{g}_\perp$ is a reciprocal lattice vector, then $-\vec{g}_\perp$ is also a reciprocal lattice vector, Eq. (III.12) becomes

$$\phi(z) = \sum_{g_\perp} \cos \vec{g}_\perp \cdot \vec{b} \; \psi(g_\perp, z) \; . \qquad \text{(III.13)}$$

In Appendix B, an expression for $\psi(g_\perp, z)$ is obtained for large by using the properties of the singularities in the integrand of the integral in Eq. (III.12). For $2k_F > g_\perp$,

$$\psi(g_\perp, z) = - \frac{\pi k_o}{2Ak_F^3} \frac{\sin 2k_o z}{(2k_F z)^2} \qquad \text{(III.14)}$$

where $2k_o \equiv \sqrt{4k_F^2 - g_\perp^2}$ as defined in Appendix B. For $2k_F < g_\perp$, $\psi(g_\perp, z)$ is a function which decays exponentially and makes little contribution to Eq. (III.13); terms with $2k_F < g_\perp$ will be neglected below.

The expressions above are valid for parallel planes of any type. However, the interplanar interaction finds its best use when the planes under consideration are hexagonal close-packed; we will now specialize to this case. The formulae for the direct space and reciprocal space lattice vectors for hexagonal close-packed planes can be found in Appendix C. We let a be the nearest neighbor distance in the plane so that

$$A = \frac{\sqrt{3}}{2} a^2 \quad \text{and} \quad \Omega = \frac{\sqrt{3}}{2} a^2 d \ . \tag{III.15}$$

It is convenient to define

$$\gamma = \frac{(d/a)}{(d/a)_{ideal}} \tag{III.16}$$

where $(d/a)_{ideal} = \sqrt{2/3}$ is the ideal axial ratio for true close-packed structures. Also of use is the definition of the value of the valence, Z_c, at which the first non-zero reciprocal lattice vector equals $2k_F$:

$$2k_F = 2\left(\frac{3\pi^2 Z_c}{\Omega}\right)^{1/3} = \frac{4\pi}{\sqrt{3}a} \tag{III.17}$$

or

$$Z_c = 1.14\gamma$$

where Eqs. (III.15) and (III.16) have been used. The next largest reciprocal lattice vector is equal to $2k_F$ when

$$Z = \sqrt{27}\, Z_c = 5.92\gamma \tag{III.18}$$

Attention will be restricted to cases where $Z < 5.92\gamma$ for the present. We have some more definitions:

$$2k_F z = 2k_F nd = n\theta'$$

with

$$\theta' = 2\left(\frac{4\pi^2}{\sqrt{3}}\right)^{1/3} Z^{1/3}\gamma^{2/3} = 5.67\, Z^{1/3}\gamma^{2/3}$$

and

$$2k_o z = 2k_o nd = 2k_F\left[1 - \frac{Z_c^{2/3}}{Z^{2/3}}\right]^{1/2} nd = n\theta$$

with

$$\theta = 2\left(\frac{4\pi^2}{\sqrt{3}}\right)^{1/3} (Z^{2/3} - Z_c^{2/3})^{1/2}\, \gamma^{2/3}$$

$$= 5.67\, (Z^{2/3} - Z_c^{2/3})^{1/2}\, \gamma^{2/3}\ .$$

With these definitions,

$$\psi(0,nd) = -\frac{.205\,\theta' \sin n\theta'}{(2\pi)^3 Z^{5/3}\gamma^{4/3} n^2} \tag{III.19}$$

$$\psi(g_1, nd) = -\frac{.205\,\theta \sin n\theta}{(2\pi)^3 Z^{5/3}\gamma^{4/3} n^2}\ . \tag{III.20}$$

Next, consider the change in energy required to shift an ion from a position directly above another ion in the lattice by an amount $\vec{b} = \frac{1}{3}(\vec{a}_2 - \vec{a}_1)$, where $\vec{a}_1$, and $\vec{a}_2$ are the direct lattice vectors of the hexagonal lattice:

$$\Delta\phi(z) = \sum_i v(|\vec{z} + \vec{b} + \vec{\rho}_i|) - v(|\vec{z} + \vec{\rho}_i|)$$

$$= \sum_{g_\perp} (\exp - i\vec{g}_\perp \cdot \vec{b} - 1)\, \psi(g_\perp, z) \qquad \text{(III.21)}$$

$$= \frac{1.84\, \theta \sin n\theta}{(2\pi)^3\, Z^{5/3} \gamma^{4/3} n^2}$$

The generalization of the interplanar interaction follows the formulation of Section III.B closely. Let the ions of the basis be at positions designated by $\vec{\sigma}$ j with respect to some origin (See Fig. 2). The displacement vector $\vec{\sigma}$ j can be decomposed into components which are perpendicular ($\zeta_j \hat{z}$) and parallel ($\vec{\beta}_j$) to the hexagonal, planar lattices:

$$\vec{\sigma}_j = \zeta_j \hat{z} + \vec{\beta}_j \qquad \text{(III.22)}$$

By letting $\vec{\rho}_i$ designate the positions of other unit cells with respect to the origin, as before, the interaction between the $j^{\underline{th}}$ ion of the original unit cell and the $j^{\underline{th}}$ ion of some other unit cell may be written as

$$V_{jj'}(r) = V_{ojj'} \frac{\cos 2k_F r}{(2k_F r)^3} \qquad \text{(III.23)}$$

where

$$r = |\vec{z} + \vec{b} + \vec{\rho}_i + \vec{\sigma}_j, - \vec{\sigma}_j|$$

$$k_F = \left(\frac{3\pi^2 Z}{\Omega}\right)^{1/3}$$

Note that

$$Z = \sum_j Z_j \qquad \text{(III.24)}$$

is the sum of all conduction electrons associated with the unit cell and

$$\Omega = \vec{a}_1 \times \vec{a}_2 \cdot (d\hat{z}) \qquad \text{(III.25)}$$

is the volume of the unit cell (See Appendix C). The vectors $\vec{b}$ and $\hat{z}$ have the same significance as in Section III.B.

For the total interaction of a unit cell and a plane composed of similar unit cells at distance z, Eq. (III.23) must be summed over i, j and j':

$$\Phi(z) = \sum_{i\ j\ j'} V_{jj'}(|\vec{z} + \vec{b} + \vec{\rho}_i + \vec{\sigma}_j, - \vec{\sigma}_j|) \qquad \text{(III.26)}$$

As with the simple interplanar interaction, it is useful to find the energy required to shift the unit cell under consideration from an equivalent to an inequivalent position with respect to the plane under consideration:

$$\Delta\Phi(z) = \sum_{ijj'} V_{jj'}(|\vec{z} + \vec{b} + \vec{\rho}_i + \vec{\sigma}_j, - \vec{\sigma}_j|) - V_{jj'}(|\vec{z} + \vec{\rho}_i + \vec{\sigma}_j, - \vec{\sigma}_j|) \qquad \text{(III.27)}$$

The sum over i in the above equation is transformed as before to obtain

$$\Delta\Phi(z) = \sum_{jj'} V_{ojj'} \sum_{k} \kappa^{k}_{jj'} \frac{1.16(Z^{2/3} - Z_{ck}^{2/3})^{1/2}}{(2\pi)^3 Z^{5/3}\eta^2} \sin \eta\theta \qquad \text{(III.28)}$$

where

$$\kappa^{k}_{jj'} = \sum_{g_\perp^k} \exp i\vec{g}_\perp^{k}\cdot(\vec{b} + \vec{\beta}_{j'} - \vec{\beta}_j) - \exp i\vec{g}_\perp^{k}\cdot(\vec{\beta}_{j'} - \vec{\beta}_j) ,$$

$$\eta = (z + \zeta_{j'} - \zeta_j)/d ,$$

and

$$Z_{ck} = 1.14\gamma, \quad 5.92\gamma, \ldots .$$

Equation (III.21) is the asymptotic form of the interplanar interaction of Blandin, Friedel and Saada in the form in which it will be used. The interaction falls off like z^{-2} compared to the r^{-3} form of the Friedel potential itself. It is interesting to compare this behavior with the Coulomb field of a charged particle and plane. Upon integration of the r^{-2} field of particles over a plane, a constant field is obtained, i.e. the dependence of the field on distance loses a factor of r^{-1} for each of the two dimensions involved in the integration. In contrast, the Friedel potential, a factor of $r^{-1/2}$ is lost for each dimension involved in the integration. Of course, the reason for this behavior is the appearance of the cosine in the Friedel potential.

Blandin et al.[6] have also found the asymptotic form for $Z<Z_c$. Around Z_c, the asymptotic forms yield poor approximations to exact sums of the Friedel potential, as will be seen below. Further, it applies

only for $Z<Z_c = 1.14$ (for ideal c/a ratio materials). For these reasons, this form will not be discussed here.

C. The Interlinear Interaction

In the last section, the energy of interaction of an ion with a planar array of ions was found. This interaction was cast in a relatively simple asymptotic form which is valid for large separations between the ion and the planar array. In this section, a similar type of interaction, between an ion and a linear array of ions, will be derived using a technique analogous to that found in the previous section. If a structure contains two parallel lines of ions, then a simple summation of the ion-line interaction in turn yields an interlinear interaction. The interlinear interaction is particularly useful in situations where there is translational symmetry in one direction only and where the structure factors are difficult to calculate, i.e., for dislocations. In fact, the interlinear interaction was originally derived and used by Rabier and Grilhe[16] to discuss a screw dislocation in a bcc lithium crystal.

Referring to Fig. 3, we assume that the ion at the origin of the coordinate system interacts according to the Friedel potential, Eq. (II.4), with each ion that forms a row a distance ρ away from the origin. The ions in the row are positioned at

$$\vec{r}_m = \rho\hat{x} + (x + md)\hat{z} \qquad \text{(III.29)}$$

where m labels the ions in the row, and d is the spacing between ions along the row. The interaction energy of the row and the ion is given by

$$\psi(\rho,z) = \sum_{m=-\infty}^{\infty} \frac{\cos 2k_F r_m}{(2k_F r_m)^3} \tag{III.30}$$

where w(k) is the inverse Fourier transform of the Friedel potential as given in Appendix A. The use of cylindrical coordinates leads to simplification of Eq. (III.18). Letting

$$\vec{k} = k_\perp \hat{r} + k_\parallel \hat{z} \tag{III.31}$$

with

$$\hat{r} = \cos\theta\hat{x} + \sin\theta\hat{y}$$
$$\hat{\theta} = -\sin\theta\hat{x} + \cos\theta\hat{y}$$
$$\hat{z} = \hat{z}$$

so that

$$\vec{k} \cdot \vec{r}_m = \rho k_\perp \cos\theta + k_\parallel (z + md) \tag{III.32}$$

Eq. (III.18) becomes

$$\psi(\rho,z) = \frac{2\Omega}{(2\pi)^3} \sum_{m=-\infty}^{\infty} \int_0^\infty dk_\perp \int_{-\infty}^{\infty} dk_\parallel \int_0^{2\pi} d\theta \tag{III.33}$$

$$k_\perp w\left(\sqrt{k_\parallel^2 + k_\perp^2}\right) \exp -i(k_\perp \rho \cos\theta + k_\parallel (z + md))$$

The structure factor for a linear array of ions is given by

$$\frac{1}{N}\sum_{m=-\infty}^{\infty} \exp -ik_{\parallel} md = \frac{2\pi}{Nd}\sum_{g_{\parallel}} \delta(\vec{k}_{\parallel} - g_{\parallel}) \qquad \text{(III.34)}$$

where $\vec{g}_{\parallel} = 2\pi m\hat{z}/d$ denotes the reciprocal lattice vectors of the line of ions. With Eq. (III.22) in Eq. (III.21), we obtain

$$\psi(\rho,z) = \frac{2\Omega}{(2\pi)^2 d}\sum_{g_{\parallel}} \exp -ig_{\parallel} z$$

$$\int_o^{\infty} dk_{\perp}\ k_{\perp}\ w\left(\sqrt{k_{\perp}^2 + g_{\parallel}^2}\right)\int_o^{2\pi} d\theta\ \exp -ik_{\perp}\rho\cos\theta \qquad \text{(III.35)}$$

Using a definition of J_o, a Bessel's function,

$$J_o(x) = \frac{1}{\pi}\int_o^{\pi} d\theta\ \exp\ ix\cos\theta\ , \qquad \text{(III.36)}$$

one obtains

$$\psi(\rho,z) = \frac{\Omega}{\pi^3 d}\sum_{g_{\parallel}} \exp -ig_{\parallel} z\ F(\rho,g_{\parallel}) \qquad \text{(III.37)}$$

where

$$F(\rho,g_{\parallel}) = \int_o^{\infty} dk_{\perp}\ k_{\perp}\ J_o(k_{\perp}\rho)\ w\left(\sqrt{k_{\perp}^2 + g_{\parallel}^2}\right)$$

Further simplification occurs if ρ is large, since use can be made of the asymptotic form of $J_o(x)$,

$$J_o(x) = \sqrt{\frac{2}{\pi x}} \cos(x - \tfrac{\pi}{4}) \qquad \text{(III.38)}$$

As with the interplanar interaction, the asymptotic form of Eq. (III.37) is determined by the singularities in w(k). One obtains

$$F(\rho,o) = \frac{\sqrt{2\pi}}{(2k_F)^{1/2}d} \frac{\sin(2k_F\rho + \frac{3\pi}{4})}{\rho^{5/2}} \qquad \text{(III.39)}$$

and

$$F(\rho,g_{\|}) = \frac{\sqrt{2\pi}\ (2k_1)^{3/2}}{(4k_F{}^2 d)} \frac{\sin(2k_1\rho + \frac{3\pi}{4})}{\rho^{5/2}} \qquad \text{(III.40)}$$

where $2k_1 = (2k_F{}^2 - g_{\|}{}^2)^{1/2}$. Again, only terms with $g_{\|} < 2k_F$ will contribute to Eq. (III.37). In the case of the interlinear interaction, this will generally mean that only the first two terms will contribute.

IV. STABILITY AGAINST PHASE TRANSFORMATION

One criterion for the stability of a crystal lattice is that it have the lowest free energy of all possible crystal lattices. The determination of the crystal lattice or structure with the minimum free energy, either empirically or theoretically, is the usual content of studies of phase stability. In this chapter, the Friedel potential will be used to test a few of the large number of possible crystal lattices to find the minimum energy lattice, i.e., the minimum free energy at T=0 K.

In the first section, the exact summation is performed for the fcc, hcp, bcc, dc (diamond cubic), and sc (simple cubic) structures to find the minimum energy structures. The axial ratio of the hcp structure is assumed ideal. The energies of the phases with respect to the fcc phase, $\varepsilon_{hcp}-\varepsilon_{fcc}$, $\varepsilon_{bcc}-\varepsilon_{fcc}$, etc., are then found by simple subtraction and are plotted as functions of Z.

As mentioned above, the application of the Friedel potential is probably most appropriate to the study of the relative energies of the close-packed polytypes structures with ideal axial ratios. The polytypes are easily and accurately handled through use of the interplanar interaction of Blandin, Friedel and Saada. In the second section, the method for the use of the interplanar interaction is developed and the relevant sums are performed. This method gives directly the energy of a polytype relative to the energy of the fcc structure, $\varepsilon-\varepsilon_{fcc}$. Using the sums, the relative energies for a number of polytypes can be plotted as functions of Z.

The relative energies may be used to determine which structure is the most stable of those considered. Plots of the regions of Z for which the different structures are preferred are presented. Up to this point, the relative stability of different structures has been considered to be determined by one variable, the electron-atom ratio Z. The actual structures exhibited by the simple metals indicate that Z is not the only determinant of structure. In an attempt to circumvent this defect of the model, two modifications of the Friedel potential are considered in the next two sections.

The first modification is the introduction of a new parameter into the Friedel potential. This parameter is a phase factor, which will subsequently be referred to as the Friedel shift, of 2δ in the argument of the cosine of the Friedel potential. The resulting potential is of the form

$$v'(r) = \frac{\cos(2k_F r + 2\delta)}{(2k_F r)^3} \qquad \text{(IV.1)}$$

When Eq. (IV.1) is used in Eq. (III.1), the dimensionless structure dependent energy depends on both the electron-atom ratio Z and the Friedel shift. The stability of the simple crystal structures has been determined as of function of Z and 2δ by modifying both the exact summation method and the method developed in the second section for summing the interplanar interaction.

The second modification considered in the final section pertains only to the application of the interplanar interaction to the stability of close-packed polytypes. Instead of simply using the interplanar interaction in Eq. (III.21), $\Delta\phi(2d)$ is adjusted to reflect conditions that might hold when the dhcp, Sm, and A polytypes occur. The regions of Z for which the complex polytypes might appear are determined under these conditions.

A. Exact Summation of the Friedel Potential

The formulae for the exact summation of the Friedel potential were developed in Chapter III. Discussed here are some considerations about the evaluation of the formulae.

The convergence parameter, ω, may be chosen arbitrarily in Eqs. (III.2) and (III.4). If $\omega=\pi/s^2$ is chosen, where s is the nearest neighbor distance, the sums converge with equal rapidity.[17] In our computations fifty or sixty lattice vectors were used for the sums on the right-hand side of Eqs. (III.2) and (III.4). Then ω was adjusted so that the last terms evaluated for the sums were about equal. It was found that ω differed from π/s^2 by a small amount and the last terms in the two sums contributed less than 10^{-4} to the expression being evaluated. An accuracy of 10^{-4} is thus claimed for these sums. The difference between π/s^2 and the final values chosen for ω is evidently due to the truncation of the sums; the value $\omega = \pi/s^2$ is applicable only to a complete summation.

In Fig. 4, the quantities ε_{fcc}, ε_{hcp}, and ε_{fcc}, as determined from exact summation, are plotted as functions of Z. In Fig. 5 are plotted the relative energies $\varepsilon_{hcp}-\varepsilon_{fcc}$, and $\varepsilon_{bcc}-\varepsilon_{fcc}$. These dimensionless energies have a magnitude of 5×10^{-3} or less for the range of Z considered. This range is taken to be from 1.00 to 4.00, the range of valence which includes the simple metals to which pseudopotential theory should apply.[1,9] The results, shown in Figs. 4 and 5 can be used to determine which of the structures has the lowest energy as a function of Z. In Fig. 6 are shown plots of ε_{fcc}, ε_{sc}, and ε_{dc} structures.

B. Summation of the Interplanar Interaction

The computation of the relative energies of the different close-packed polytypic structures can be done without the exact evaluation of Eq. (III.2). The method for doing this calculation uses an approximate interplanar interaction between two parallel, hexagonal close-packed planes developed in Section III.B. In particular, close-packed polytypic structures can be described as the stacking of hexagonal, close-packed planes of three types, A, B, or C. When these planes are considered pairwise, they are in either equivalent (e.g., A-A) or inequivalent (e.g., A-B) positions. For example, the stacking sequence of the fcc structure is ABCABC; the first and fourth planes in the stacking sequence are in equivalent positions, while the first and second planes and the first and third planes are in inequivelent positions. The interplanar interaction of Blandin, Friedel and Saada

is a rearrangement interaction which gives the change in energy when two parallel, hexagonal close-packed planes are shifted from equivalent to inequivalent positions. The expression for $\Delta\phi(z)$ given in Eq. (III.21) is just this energy and will be denoted $\Delta\phi^{BFS}(nd)$ in this chapter (Z=nd).

Following a suggestion by Hodges,[10] the $\Delta\phi^{BFS}(nd)$ of Section III.B can be used to calculate the structure-dependent energy and relative stability of any close-packed structure. Let c_n be the fraction of $n^{\underline{th}}$ nearest neighbor planes in equivalent positions for some structure. For example, c_1 equals zero for any structure, since nearest neighbor planes are always in inequivalent positions. The structure-dependent energy per atom of some structure with respect to the fcc structure is just

$$\varepsilon-\varepsilon_{fcc} = \sum_{n=1}^{\infty} \Delta c_n \, \Delta\phi(nd) \qquad \text{(IV.2)}$$

where $\Delta c_n = c_n^{fcc} - c_n$, and c_n is the coefficient of the phase in question. Table II shows stacking characteristics and stacking sequences for the polytypic structures considered in this paper.

When Eq. (III.21) is used in Eq. (IV.2) for $Z > Z_c$, one can obtain a simplification by noting that Δc_n is periodic in n. If (nd) is a common repeat distance for the structure in question and the fcc structure, we can rewrite Eq. (IV.2) as

$$\varepsilon-\varepsilon_{fcc} = \sum_{n'=0}^{\infty} \sum_{k=1}^{j} \Delta c_{jn'+k} \; \Delta\phi((jn' + k)d)$$

$$= \sum_{n'=0}^{\infty} \sum_{k=1}^{j} \Delta c_{k} \; \Delta\phi((jn' + k)d) \qquad \text{(IV.3)}$$

$$= \sum_{k=1}^{j} \Delta c_{k} \sum_{n'=0}^{\infty} \Delta\phi((jn' + k)d)$$

For example, it is found that the hcp structure has an energy of

$$\varepsilon_{hcp}-\varepsilon_{fcc} = \sum_{n=0}^{\infty} \Delta\phi((6n+3)d) - \Delta\phi((6n+2)d) + \Delta\phi((6n+4)d) \qquad \text{(IV.4)}$$

with respect to the fcc structure. The terms $\sum_{n'=0}^{\infty} \Delta\phi((jn'+k)d)$ in Eq. (IV.3) can be easily evaluated when Eq. (III.21) is used. It is shown in Appendix D that

$$\sum_{n=0}^{\infty} \Delta\phi^{BFS}((jn+k)d) \propto \sum_{n=0}^{\infty} \frac{\sin(jn+k)\theta}{(jn+k)^2}$$

$$= \frac{1}{j} \sum_{\ell=0}^{j=1} \sin \frac{2\pi k\ell}{j} \beta_2(\theta+\frac{2\pi\ell}{j}) + \cos \frac{2\pi k\ell}{j} \alpha_2(\theta+\frac{2\pi\ell}{j}) \qquad \text{(IV.5)}$$

where

$$\alpha_2(\theta) = \sum_{n=1}^{\infty} \frac{\sin n\theta}{n^2} = -\theta \ \ell n \ 2\left|\sin \frac{\theta}{2}\right| + 2 \int_o^{\theta/2} \frac{\phi d\phi}{\tan\phi}$$

and

$$\beta_2(\theta) = \sum_{n=1}^{\infty} \frac{\cos n\theta}{n^2} = \frac{\theta^2}{4} - \frac{\pi\theta}{2} + \frac{\pi^2}{6}$$

The function α_2 was obtained numerically to six digit accuracy using polynomial expansions with six terms. This accuracy is needed to assure significance in the evaluation of Eq. (IV.5) when used in Eq. (IV.3).

Use of Eq. (IV.5) in Eq. (IV.3) allows a simple calculation of $\varepsilon-\varepsilon_{fcc}$. The method does not require the calculation of reciprocal lattice vectors as in the exact summation method and is easily visualized. The results for $\varepsilon_{hcp}-\varepsilon_{fcc}$ using the interplanar interaction are shown in Fig. 7 as a function of the valence.

Results for three polytype structures are also displayed in Fig. 7. Two of these, the double hexagonal (dhcp) and samarium (Sm) structures, are occastionally observed experimentally. In terms of Pauling's h-k notation (Table II) these structures have one half and two thirds hexagonal character, respectively. The final structure, designated the A structure, has one third hexagonal character and is included for completeness. These complex polytypes might be considered as compromise structures that occur when the fcc and hcp structures have nearly the same energies. Table II summarizes the stacking characteristics of these complex polytypes.

The odd behavior of the interplanar interaction near Z = 1.14 shows up clearly in Fig. 7. Using the results from the exact summation, the values of $\varepsilon_{hcp}-\varepsilon_{fcc}$ from the two methods can be compared and are plotted in Fig. 8. The exact summation yields $\varepsilon_{hcp}-\varepsilon_{fcc} \neq 0$ at Z = 1.14.

This result implies that there should be non-zero terms in Eq. (IV.2), i.e., the interplanar interaction is not always zero at Z=1.14. Evidently, the approximate interplanar interaction breaks down near this value of Z. It is of interest to note the good agreement between the results of the two methods at other values of the valence.

C. Inclusion of a Phase Factor in the Friedel Potential

The Friedel oscillations were originally derived as oscillations in the charge density surrounding an ion in an electron gas.[18] A Friedel shift appears in the result for the charge density, as in Eq. (IV.1). However, as usually derived from pseudopotential theory carried to second order in perturbation theory,[1] neither the charge density oscillations nor the Friedel potential contain a Friedel shift. Only in higher orders of perturbation theory does the Friedel shift occur. Friedel,[19] Seeger,[20] Heine and Weaire,[8] and Harrison[21] have also discussed the significance of the Friedel shift. Although it is not yet clear what role the Friedel shift plays in interionic potentials, the present formulation alloys the Friedel shift to be incorporated into the determination of structure in a simple way, and this is done below. To sum the potential, Eq. (IV.1), over the lattice as in Eq. (II.7), we note that Eq. (IV.1) can be decomposed into the form

$$v(r) = \cos 2\delta \frac{\cos 2k_F r}{(2k_F r)^3} - \sin 2\delta \frac{\sin 2k_F r}{(2k_F r)^3} \quad . \qquad \text{(IV.6)}$$

Now just as Eq. (II.7) could be summed using Shaw's development of Epstein's method, the term $\sin(2k_Fr)/(2k_Fr)^3$ can be summed using a Eq. (III.7).

The term $\sin(2k_Fr)/(2k_Fr)^3$ can also be cast into the form of an interplanar interaction, just as was done by Blandin et al. for the term $\cos(2k_Fr)/(2k_Fr)^3$. Instead of a singularity of the type $(k-2k_F)\ln|k-2k_F|$, a form like $|k-2k_F|$ appears. The final result is to simply add a Friedel shift to the interplanar interaction:

$$\Delta\phi(nd) = 10.44 \frac{V_0(1 - (Z/Z_c)^{2/3})^{1/2}}{(2\pi)^3 Z^{4/3}} \frac{\sin(n\theta + 2\delta)}{n^2} \qquad \text{(IV.7)}$$

Expressions (IV.1) and (IV.7) can now be used in Eqs. (II.7) and (IV.2) to determine the stable structure just as before, except that this structure will be a function of both Z and 2δ. This information can then be used to determine which structure, of those considered, is most stable as a function of the two variables. Figures 5 and 6 show the structures found to be preferred when a Friedel shift is included in the Friedel potential. Figure 5 is the result of the exact summation technique. Only the fcc, hcp and bcc structures were considered in this determination. Figure 5 shows which of the structures, fcc, hcp, dhcp, Sm, or A, are preferred as a function of Z and 2δ as determined by Eqs. (IV.1) and (IV.7).

D. Alternate Criteria for the Occurrence of Complex Close-Packed Polytypes

In this section, the model presented above is modified in a second way to obtain values of Z for which complex polytypes might be found. In particular, the interplanar interaction, with adjustment of $\Delta\phi(2d)$, is used to obtain the regions of Z where the polytypes dhcp, Sm, and A might occur. What is recognized is that, since the interplanar interaction of Blandin, Friedel and Saada may be in error for small separations, $\Delta\phi^{BFS}(2d)$ may not necessarily be a good approximation to the actual interplanar interaction for second nearest neighbor planes. $\Delta\phi(2d)$ is hence adjusted to meet other requirements.

The dhcp, Sm and A structures (Table II) may be considered to be compromise structures occurring when the fcc and hcp structures have nearly the same energy. This condition can be simulated by either setting $\Delta\phi(2d) = 0$, as was done by Hodges,[10] or by requiring that $\varepsilon_{fcc} = \varepsilon_{hcp}$ and adjusting $\Delta\phi(2d)$ accordingly. These two criteria for the appearance of the complex polytypes are investigated below.

The condition that Hodges[10] used for the appearance of complex close-packed polytypes is of the form

$$\Delta\phi(2d) = 0$$

$$\Delta\phi(nd) = \Delta\phi^{BFS}(nd) \qquad n \geq 3 \qquad \text{(IV.8)}$$

This condition assumes that the interplanar interaction shows no preference for equivalent or inequivalent planes at the second nearest neighbor plane position. If equivalent planes are preferred at the second nearest neighbor position ($\Delta\phi(2d) > 0$), the hcp structure is favored by $\Delta\phi(2d)$, and if inequivalent planes are preferred ($\Delta\phi(2d) < 0$), the fcc structure is favored. Equation (IV.8) expresses the condition that neither type of plane is favored, so that complex polytypes, which have both types of planes at the second nearest neighbor plane position, may appear.

The values of $\Delta\phi(nd)$ from Eq. (IV.8) are to be inserted in Eq. (IV.2) to determine the preferred structure and, in particular, to determine if a complex polytype is preferred. Hodges did not evaluate the complete sums, Eq. (IV.2) and therefore could not make definite conclusions about the relative energy of the samarium structure; he did not consider the A structure. The complete sums have been done, and it is found that the energies of the dhcp and Sm structures are usually very close to one another, so that care must be taken in evaluating the sums.

The value of $\Delta\phi(2d)$ can be adjusted in another way. Rather than setting $\Delta\phi(2d) = 0$, one can set $\varepsilon_{hcp} = \varepsilon_{fcc}$ in Eq. (IV.2) by adjusting $\Delta\phi(2d)$. The other terms, $\Delta\phi(nd)$, are then taken from Eq. (III.21). This procedure has the advantage that the condition for the appearance of complex polytypes is simply stated as a condition on the relative energies of the fcc and hcp structures. However, the term $\Delta\phi(2d)$ must still be singled out for special treatment. We take

$$\Delta\phi(2d) = \Delta\phi^{o}(2d)$$
$$\Delta\phi(nd) = \Delta\phi^{BFS}(nd) \quad \text{for} \quad n \geqslant 3 \tag{IV.9}$$

where $\Delta\phi^{o}(2d)$ is adjusted in Eq. (IV.2) so that $\varepsilon_{hcp} = \varepsilon_{fcc}$. This condition with Eq. (IV.2) can be recast in the form

$$\varepsilon - \varepsilon_{fcc} = \Delta c_2(\varepsilon^{BFS}_{hcp} - \varepsilon^{BFS}_{fcc}) + (\varepsilon^{BFS} - \varepsilon^{BFS}_{fcc}) \tag{IV.10}$$

where the polytype with the minimum value of ε is preferred. Since $\Delta c_2^{hcp} = -1$, $\varepsilon_{hcp} = \varepsilon_{fcc}$, as promised.

Equation (IV.10) can be interpreted in the following way. We expect the compromise polytype structures, dhcp, Sm and A to appear when $\varepsilon_{hcp} \approx \varepsilon_{fcc}$. One can then find what value $\Delta\phi(2d)$ assumes in this case. For some values of Z, polytypes will intrude when this value of $\Delta\phi(2d)$ is used. For other values of Z, the other interactions, $\Delta\phi^{BFS}(nd)$ with $n>3$, stabilize both the fcc and hcp structures with respect to the polytypes.

V. LATTICE VIBRATIONS

Any infinitesimal deformation of a crystal lattice can be regarded as a linear combination of the extended normal mode deformations, which, when excited, are referred to as phonons. If all of the normal mode or phonon frequencies of oscillation are found to be real, then the lattice is stable against any infinitesimal deformation. Otherwise, any normal mode with an imaginary frequency can grow in amplitude with time, and the lattice will eventually relax to another configuration. Evidently, the condition that phonon frequencies be real provides another criterion for the structural stability of a lattice.

There are two other aspects of structural stability that are addressed by the study of phonons. First, lattice vibrations contribute to the free energy of a lattice through both the energy and entropy associated with vibrational modes excited at finite temperature. While this aspect of the problem will not be considered further here, these effects must be included in any study of the dependence of stability on temperature. Secondly, stability criteria have been expressed in terms of the elastic constants of a metallic crystal by Born.[22] The elastic constants are determined by the long wavelength behavior of the phonons. The criteria involve the stability of the lattice against homogeneous deformations and will be discussed in Chapter VII.

The calculation of phonon dispersion relations is particularly easy to accomplish with the interplanar interaction. As in other cases, the reason the calculation proceeds so easily is that the formulation

is essentially one dimensional in character and can be applied only to phonons propagating along symmetry directions in the lattice. Since results obtained with the asymptotic interplanar interaction only approximate those obtained with the Friedel potential, some modifications to the dispersion curves can be expected when the Friedel potential is used. In fact, since near neighbor interactions enter calculations of phonon dispersion relations, and it is in this region where the interplanar interaction fails to approximate the Friedel potential, the phonon dispersion relations calculated below are likely to be the least accurate of the calculations performed here. In other words, agreement with results from the Friedel potential, full pseudopotential calculations or experiment is not likely to be achieved below. The value of using the interplanar interaction is in its interpretive value. Koenig[23] first considered the possibility of using an interplanar interaction derived from the Friedel potential to interpret the interplanar force constants derived from experimental work. Unfortunately, his development was incomplete; some of the loose ends will be tracked down in what follows.

A. Phonon Dispersion

In order to proceed with the calculation of phonon dispersion relations along symmetry directions of metallic crystal lattices, two new approximations must be made. First, use is made of the Born-Oppenheimer approximation, whereby the positions of the ions are assumed to be the determinants of the energy of the crystal lattice.

This approximation is a very good one and rests on the fact that the electrons in a solid relax in response to a perturbation of the positions of the ions of the lattice much faster than the perturbation can be applied. The second approximation that is used is the harmonic approximation, in which it is assumed that restoring forces vary linearly with displacement. For arbitrarily large displacements, this approximation is bad, but for infinitesimally small displacements about an equilibrium configuration, the approximation is rigorously true. It is the latter case that will be considered below.

For vibrations propagating along certain symmetry directions of a crystal, the normal modes are polarized into one purely longitudinal and two purely transverse components.[3] For a given wavelength and polarization, a mode may be considered to consist of whole planes of ions vibrating either parallel or perpendicular to the propagation direction. With the introduction of interplanar stiffness constants,[3,5] the problem of determining dispersion relations becomes equivalent to a one dimensional vibration problem. The dispersion relation becomes

$$\omega^2 = \frac{1}{M} \sum_{p\neq 0} C_p(1 - \cos qpd) \qquad (V.1)$$

where ω is the angular frequency associated with the phonon of wave vector q, M is the mass of the ion, d is the interplanar spacing, and C_p is the stiffness constant between a plane serving as an origin and a parallel plane a distance pd from the origin. Equation (V.1) is particularly useful since the values of C_p can be directly determined from the interplanar interaction discussed in Chapter III. Below,

only transverse phonons propagating perpendicular to the close-packed planes of fcc and hcp lattices will be considered. While this limitation will give a somewhat narrow view of the topic, the qualitative form of dispersion relations arising from the interplanar interaction can be displayed with this type of mode. Also, these modes are related to the stability of polytypes against phase transformation as discussed in the previous chapter and the fault energies calculated in the next. All of these phenomena involve a shear across close-packed planes.

The expressions for the values of C_p in Eq. (V.1) must be found first. For a translation $\vec{\delta} = \delta\hat{\delta}$ of a plane a distance pd from a plane serving as an origin, Eq. (III.13) gives a change in energy per ion of

$$\delta\phi(z) = \sum_{g_\perp} (\cos(\vec{g}_\perp \cdot (\vec{b}+\vec{\delta})) - \cos(\vec{g}_\perp \cdot \vec{b}))\psi(g_\perp, z) \qquad (V.2)$$

for translations transverse to the stacking direction, and

$$\delta\phi(z) = \sum_{g_\perp} \cos(\vec{g}_\perp \cdot \vec{b})(\psi(g_\perp, z+\delta) - \psi(g_\perp, z)) \qquad (V.3)$$

for translations parallel to a stacking direction. As introduced in Section IV.B, the vector $\vec{b}$ is determined by whether or not the two planes are in equivalent positions with respect to each other. For small values of δ, Eq. (V.3) may be expanded in a Taylor series about $\delta=0$:

$$\delta\phi(pd+\delta) = \delta\phi(pd) + \frac{\partial}{\partial\delta}\delta\phi(pd)\ \delta + \frac{1}{2}\frac{\partial}{\partial\delta^2}\delta\phi(pd)\ \delta^2 + \ldots,$$

and similarly for Eq. (V.2).

Now the first term of the above series vanishes identically. When summed over all planes, the second term must also vanish identically, otherwise the plane under question will distort in such a way as to lower the energy of the lattice; for transverse distortions, $\frac{\partial}{\partial\delta}\,\delta\phi(z)$ does vanish. If the structure is hcp or fcc, it is also easy to see that a sum over all planes will yield zero by symmetry. It is probable that this result holds more generally. The third term yields the interplanar force constant:

$$C_p = \frac{\partial^2}{\partial\delta^2}\,\delta\phi(pd) \tag{V.5}$$

Applying Eq. (V.5) to the expressions for $\delta\phi(z)$, we obtain

$$C_p = -\sum_{g_\perp} (\vec{g}_\perp \cdot \hat{\delta})^2 \cos\vec{g}_\perp \cdot \vec{b}\; \psi(g_\perp, pd) \tag{V.6}$$

for transverse deformations. It turns out that Eq. (V.6) does not depend on the direction $\hat{\delta}$. Equation (V.6) simplifies to

$$C_p = \begin{cases} \frac{8\pi^2}{a^2}\,\psi(g_\perp, pd) & \vec{b} = \frac{1}{3}\,(\vec{a}_2 - \vec{a}_1) \\ \frac{-16\pi^2}{a^2}\,\psi(g_\perp, pd) & \vec{b} = 0 \end{cases} \tag{V.7}$$

where, in the first case, C_p is independent of the direction of $\vec{b}$ as long as $\vec{b}$ carries the $p^{\underline{th}}$ plane from an equivalent to an inequivalent position. Now $\psi(g_\perp, pd)$ is given by Eq. (III.14):

$$\psi(g_{\perp},pd) = \frac{-.205\ \theta\ \sin p\theta}{(2\pi)^3 Z^{5/3}\gamma^{4/3}p^2} \qquad (V.8)$$

where Z is the valence, $\theta = 5.67(Z^{2/3}-Z_c^{2/3})^{1/2}$, $\gamma = (d/a)/(d/a)_{ideal}$, and $Z_c = 1.14\gamma$.

Insertion of Eqs. (V.7) and (V.8) into Eq. (V.1) yields

$$\omega^2 = \frac{2}{M}\left(\frac{8\pi^2}{a^2}\right)\left(\frac{-.205\theta}{(2\pi)^3 Z^{5/3}\gamma^{4/3}}\right)$$

$$\left(-2\sum_{p=1}^{\infty}\frac{\sin 3p\theta}{(3p)^2}\ (1-\cos 3pqd)\right.$$

$$+\sum_{p=1}^{\infty}\frac{\sin(3p-1)\theta}{(3p-1)^2}\ (1-\cos(3p-1)qd)$$

$$\left.+\sum_{p=1}^{\infty}\frac{\sin(3p-2)\theta}{(3p-2)^2}\ (1-\cos(3p-2)qd)\right) \qquad (V.9)$$

$$= \frac{2}{M}\left(\frac{8\pi^2}{a^2}\right)\left(\frac{-.205\theta}{(2\pi)^3 Z^{5/3}\gamma^{4/3}}\right) \cdot$$

$$\left(-3\sum_{p=1}^{\infty}\frac{\sin 3p\theta}{(3p)^2}\ (1-\cos 3pqd)\right.$$

$$\left.+\sum_{p=1}^{\infty}\frac{\sin p\theta}{p^2}\ (1-\cos pqd)\right) \cdot$$

Noting that

$$\sin\alpha\cos\beta = \frac{1}{2}\left(\sin(\alpha+\beta) + \sin(\alpha-\beta)\right), \qquad (V.10)$$

one finds that

$$\omega^2 = \frac{2}{M}\left(\frac{8\pi^2}{a^2}\right)\left(\frac{.205\theta}{(2\pi)^3 Z^{5/3}\gamma^{4/3}}\right) \cdot \tag{V.11}$$

$$(\alpha_2(\theta) - \tfrac{1}{2}\alpha_2(\theta + qd) - \tfrac{1}{2}(\theta - qd)$$

$$- \tfrac{1}{3}\alpha_2(\theta') + \tfrac{1}{6}\alpha_2(\theta' + q'd) + \tfrac{1}{6}\alpha_2(\theta' - q'd))$$

where $\theta' = 3\theta$ and $q' = 3q$. This is the form for the dispersion relation for transverse phonons propagating in a ⟨111⟩ direction in a face-centered cubic crystal.

Similarly, we obtain

$$\omega^2 = \frac{2}{M}\left(\frac{8\pi^2}{a^2}\right)\left(\frac{-.205\theta}{(2\pi)^3 Z^{5/3}\gamma^{4/3}}\right) \cdot$$

$$\left(-2\sum_{p=1}^{\infty}\frac{\sin 2p\theta}{(2p)^2}(1 - \cos 2pqd)\right.$$

$$\left.+\sum_{p=1}^{\infty}\frac{\sin(2p-1)\theta}{(2p-1)^2}(1-\cos(2p-1)qd)\right)$$

$$= \frac{2}{M}\left(\frac{8\pi^2}{a^2}\right)\left(\frac{-.205\theta}{(2\pi)^3 Z^{5/3}\gamma^{4/3}}\right) \cdot \tag{V.12}$$

$$\left(-3\sum_{p=1}^{\infty}\frac{\sin 2p\theta}{(2p)^2}(1 - \cos 2pqd)\right.$$

$$\left.+\sum_{p=1}^{\infty}\frac{\sin p\theta}{p^2}(1 - \cos pqd)\right)$$

for transverse modes propagating parallel to a ⟨001⟩ direction in a hcp lattice. With the identity Eq. (V.10), we have

$$\omega^2 = \frac{2}{M}\left(\frac{8\pi^2}{a^2}\right)\left(\frac{.205\theta}{(2\pi)^3 Z^{5/3}\gamma^{4/3}}\right) \quad . \tag{V.13}$$

$$\left(\alpha_2(\theta) - \frac{1}{2}\alpha_2(\theta+qd) - \frac{1}{2}\alpha_2(\theta-qd)\right.$$

$$\left. - \frac{3}{4}\alpha_2(\theta') + \frac{3}{8}\alpha_2(\theta'+q'd) + \frac{3}{8}(\theta'-q'd)\right)$$

where $\theta'=2\theta$ and $q'=2q$.

For longitudinal deformations, Eq. (V.5) yields

$$C_p = \sum_{g_\perp} \cos\vec{g}_\perp \cdot \vec{b}\ \left(\frac{\partial^2}{\partial z^2}\ \psi(g_\perp, z)\right)_{z=pd} \tag{V.14}$$

and analysis similar to that found in Eqs. (V.9) to (V.14) can be applied to obtain the dispersion relations for the longitudinal vibrational modes.

Use of Eqs. (V.11) and (V.13) has been made to plot the dispersion relations for the fcc and hcp structures in Figs. 11 and 12, respectively. The maximum value of q in a close-packed direction which is inside the first (extended) Brillouin zone is just π/d where d is the interplanar spacing. The interplanar interaction was expressed in terms of dimensionless energy units in Eq. (V.2). To obtain the proper units for ω, the factor V_o must be reinserted to obtain

$$\omega^2 \sim \frac{V_o}{Ma^2} \sim \frac{\text{mass (length/time)}^2}{\text{mass}\cdot\text{length}^2} \sim \frac{1}{\text{time}^2} \quad .$$

The quantity ω will be plotted in dimensionless units, i.e.,

$$\frac{Ma^2\omega^2}{V_o} = f(z)$$

where f(z) depends on Z above, and the quantity ω' can be defined as

$$\omega' = \frac{\omega}{(V_o/Ma^2)^{1/2}}$$

In Figs. 13 and 14 are plotted the dispersion relations for ⟨001⟩T phonons in magnesium and ⟨111⟩T phonons in aluminum, respectively.[24,25] The values of V_o for the calculated curves were taken from Appapillai and Williams[26] (See Table I). For the optical branch in magnesium and large q range in aluminum, marked discrepancies in the general behavior of experimental and calculated curves occur. The behavior of dispersion curves in these regions of q is related to the short range bonding in a crystal; the discrepancies indicate that short range bonding is probably poorly modelled by the Friedel potential, a not unexpected result. In fact, most fcc dispersion curves show ⟨111⟩T behavior which is dominated by C_1 (cf. Eq. V.1), the contribution to the dispersion curves from the first nearest neighbor plane.

B. Elastic Constants

In the long wavelength limit, the vibrational modes of a solid only indirectly reflect the discrete crystal lattice of ions which compose the metallic alloy. The behavior of low frequency, long wavelength sound waves can be understood by approximating the crystal as an elastic continuum, i.e., with no discrete character. The parameters characterizing this behavior are macroscopic quantities--the density and elastic constants of the alloy. For example, the dispersion relations for phonons propagating parallel to a cube edge of a crystal with cubic symmetry become

$$\omega^2 = \frac{C_{11}}{\rho} q^2 \tag{V.15}$$

and

$$\omega^2 = \frac{C_{44}}{\rho} q^2$$

for longitudinal and transverse waves, respectively. The quantities C_{11} and C_{44} are elastic constants, and ρ is the density of the solid. By expanding the dispersion relations in the previous section about q=0, one easily obtains a similar form and the elastic constants can then be obtained from the derivatives of $\alpha_2(\theta)$

$$\omega^2 \cong \text{constant} \cdot \left[\left(-\frac{1}{2} q^2\right)\left(\frac{d^2\alpha_2(\theta)}{d\theta^2}\right) + \left(\frac{3}{2} q^2\right)\left(\frac{d^2\alpha_2(\theta')}{d\theta'^2}\right)\right] \tag{V.17}$$

For the two dispersion relations plotted in Figs. 13 and 14, two elastic constants are obtained:

$$C_{66} = 1.3\times10^{11} \frac{dy}{cm^2}$$

for magnesium and

$$(C_{11}-C_{12}+C_{44})/3 = 1.4\times10^{11} \frac{dy}{cm^2}$$

for aluminum. These values show reasonable agreement with the experimental values of 1.64×10^{11} dy/cm^2 and 2.34×10^{11} dy/cm^2, respectively, although this agreement depends on the pseudopotential form factor used to calculate V_o. What is of interest is that experimental values can be approximated by using the Friedel potential, which is just the long range part of any interatomic potential arising in pseudopotential theory.

VI. FURTHER ASPECTS OF STABILITY

In this chapter, two other facets of the study of stability are introduced: the stability against the formation of stacking faults and twins, and the stability of lattices against finite homogeneous deformations.

A. Stacking Faults and Twins

The defect structure of a metallic alloy is one of the principal determinants of mechanical properties. The properties of dislocations, obstacles to dislocation glide, grain boundaries, etc., all influence how the metal behaves under stress. Unfortunately, the problem of sorting out the influences of these defects on mechanical properties is and will remain an immense theoretical and experimental task, although progress is being made by a number of careful workers. One type of defect, the coherent planar fault, has received much attention over the last decade. Planar faults, be they stacking faults or twins, are characterized by a disturbance of the regular stacking of planes in a metallic crystal and have received both experimental and theoretical attention for two reasons. First, fault energies are not too difficult to either measure or calculate.[27] The agreement between theoretical and experimental estimates of stacking fault energies is fairly good, although there is probably a factor of two difference between these two estimates or between these estimates and the true values of stacking fault energies of actual metals. Secondly, the stacking fault energy

appears to be an important parameter in the characterization of the plastic deformation of close-packed materials, and hence has possible practical significance in the study of the mechanical properties of metals.

The stability of close-packed metallic crystals against the formation of stacking faults and twins, rather than the mechanical properties of the alloys, will be discussed below. In terms of our categorization of deformations in the Introduction, a stacking fault is a localized, inhomogeneous distortion of a perfect crystal lattice. In close-packed metals, twins and stacking faults lie parallel to close-packed planes, i.e., {111} planes in fcc structures and {001} planes in hcp structures. This orientation makes the calculation of fault energies amenable to the use of the interplanar interaction derived in Chapter III. In fact, Blandin et al.[6] originally formulated the interplanar interaction to treat these types of fault.

Several types of notation exist for the description of planar faults. The convention that will be used here is the same used to describe polytypes in Chapter IV. Thus, the letter k will describe a plane with an environment of cubic symmetry, i.e., with neighboring planes in inequivalent positions and an h will designate a plane in a hexagonal environment of two neighboring planes in equivalent positions. For the fcc and hcp lattices, there are three common types of planar fault: the intrinsic and extrinsic stacking faults and the twin fault. In the fcc lattice, two hexagonal type layers are found in the stacking of a crystal containing either an intrinsic or an

extrinsic fault, as can be seen from Table IV. Likewise, a twin gives rise to only one hexagonal type layer. In an hcp material the intrinsic, extrinsic and twin faults give rise to two layers, three layers, and one layer with cubic symmetry, respectively. Other types of faults can be visualized; in fact, E. A. Harrison[28] has treated a number of different types of planar faults in aluminum. Also, different types of faults will arise when polytypes other than the fcc and hcp structures are considered. Attention will be restricted to the faults already delineated.

A simple model[27] for the energies of the different types of fault can be constructed using an interaction between second nearest neighbor planes only. If Δ is the difference in energy between planes in equivalent and in inequivalent positions, then the energies of intrinsic, extrinsic and twin faults are 2Δ, 2Δ, and Δ in the fcc structure and -2Δ, -3Δ and $-\Delta$ in the hcp structure. Similarly, the difference in energy between the hcp and fcc structures is just Δ per plane of material. This model neglects forces of range further than twice the interplanar spacing and will be refined below to include some of the long range effects.

In their treatment of stacking faults, Blandin et al.[6] developed the formulae needed to deal with the long-range interplanar interaction developed in Chapter III. With the $\Delta\phi(nd)$ defined above, the fault energies are given by:

face-centered cubic: $\Delta\varepsilon =$

intrinsic: $$\sum_{n=1}^{\infty} [3n\ \Delta\phi(3nd) - (3n-1)\ \Delta\phi((3n-1)d)]$$

extrinsic: $$\sum_{n=1}^{\infty} [(3n+1)\Delta\phi(3nd) - 3n\Delta\phi((3n+1)d) - 2\Delta\phi((3n-1)d)]$$

twin: $$\sum_{n=1}^{\infty} n[2\Delta\phi(3nd) - \Delta\phi((3n-1)d) - \Delta\phi((3n+1)d)]$$

hexagonal close-packed:

intrinsic: $$\Delta\varepsilon = \sum_{r=1}^{\infty} n[2\Delta\phi(2nd) - \Delta\phi((2n+1)d)]$$

extrinsic: $$\sum_{n=1}^{\infty} [(2n+1)\Delta\phi(2nd) - 2n\Delta\phi((2n+1)d)]$$

twin: $$\sum_{n=1}^{\infty} [n\Delta\phi(2nd)]$$

Since the interplanar interaction has been expressed in dimensionless units, a factor of $V_o/(\sqrt{3}a^2/2)$ must be inserted to yield proper dimensions-erg/cm^2. The generalization of the interplanar interaction to include arbitrary c/a ratios also allows the various fault energies to be calculated as a function of c/a. This has been done for Z=2 and in Fig. 15, the results for the hcp lattice at Z=2 can be found.

The sums over combinations of $\Delta\phi(nd)$ above can be evaluated in terms of functions like $\alpha_2(\theta)$ and $\beta_2(\theta)$ defined in Chapter IV; Blandin et al.[6] give the details of the computation. These formulae reduce to the simple model results given above, if values of $\Delta\phi(nd)$ with n greater than two are neglected.

B. Finite Homogeneous Deformations

With either the exact summation method of the Friedel potential or the interplanar interaction, the highly symmetrical crystal structures considered in Chapter IV can be subjected to finite homogeneous deformations. All that need be done is vary the crystal structure to simulate the deformation.

The relationship between finite deformations and other aspects of stability has not been explored fully; the purpose of this section is to point out that finite deformations can be investigated with the present formalism and that they are intimately related to the other aspects of the study of the stability of structures.

In Fig. 17 are plotted the results of a calculation of the dimensionless energy, ε, as a function of the c/a ratio of a body-centered tetragonal (bct) lattice as calculated from Eq. (III.6). At c/a = 1.414, the bct structure is equivalent to the fcc structure as indicated in Fig. 16. The curvature of the curves for ε in Fig. 17 is proportional to the elastic constant $(C_{11}-C_{12})/2$ and, in fact, use of these calculations could be made to obtain the results of Cousins[29] for the elastic constants $(C_{11}-C_{12})/2$ and C_{44}.

Another aspect of theoretical studies of lattice stability is illustrated in Fig. 17. The Born stability criteria are that

$$C_{11}-C_{12} > 0 \quad \text{and} \quad C_{44} > 0$$

for cubic crystals. These conditions apply only to the curvature of the energy as a function of some deformation parameter. For a theoretical model of a metal, there is no guarantee that no contribution to the energy which is linear with the deformation enter, unless additional constraints are put on the lattice. Such linear terms can obviously cause minima in energy to be found for structures other than the bcc and fcc structures. What is of interest is that in Fig. 17, where there is a positive value of $(C_{11}-C_{12})/2$ for the bcc and fcc structures, there also occur local minima of the energy for these structures.

VII. THE STABILITY OF CRYSTAL LATTICES

In the preceding chapters, a number of quantities have been calculated with the Friedel potential. It is easily argued that the Friedel potential leaves much to be desired as an interatomic potential. At both short and long ranges, the bonding is probably not well represented by the Friedel potential. On the other hand, it can also be argued that the value of the Friedel potential is due, in some sense, to its uniqueness. The strength of what has been calculated above lies not so much in its agreement with experimentally determined quantities as in that a particular facet of pseudopotential theory has been investigated in some detail. The results obtained above are summarized and interpreted below.

A. Interpretation of Structural Energies

In Chapter IV, a number of computations of structural energies of crystal lattices were performed using the Friedel potential. Below, these energies will be discussed in terms of the form of the Friedel potential at various values of the valence. Following this discussion, the results of Chapter IV are considered in relation to the assumptions used to obtain the Friedel potential and in relation to actual phases found in simple metal systems.

It has been noted that the Friedel potential, Eq. (II.6), is independent of volume. Using the completely dimensionless form found in Section III.A, the Friedel potential has been plotted in Fig. 18

for Z = 1 to 4. Also shown in the figure are positions of the first nearest neighbors of an ion for several different crystal structures. The Friedel potential itself is oscillatory in nature with an envelope that decreases with distance like $1/r^3$. For fixed Z, the potential exhibits a repulsive region as r increases, then a local minimum in which the nearest neighbor ion of some ion might be expected to prefer to be positioned, and then a maximum. There is actually another minimum of the Friedel potential at smaller values of r, but it is spurious in the sense that it will not appear in an interionic potential derived from the full theory. Instead, this region of r, which corresponds to a large overlap of the cores of the ions, should be characterized by an increasingly large repulsive interaction. As Z increases the oscillations contract and appear at smaller values of r.

The near neighbor interactions might be expected to dominate the behavior of the energies of the various crystal structures available to the metallic alloy. This behavior is reflected to some extent in Figs. 4 and 6, where the results of summing Eq. (II.6) for various crystal crystal structures is displayed as a function of Z. In Fig. 4, the results for bcc, fcc, and hcp lattices are plotted. All of the curves show a sharply decreasing and positive energy, then a minimum, and then a slow rise. This behavior is easily understood in terms of Fig. 18 in which, as Z is increased, the first nearest neighbor vectors "slide down" the repulsive region into the minimum and up the adjoining maximum. Figure 6 displays similar results for the fcc, simple cubic and diamond cubic structures. These curves cannot display

realistic behavior for low values of Z because the first nearest neighbors are affected by the first, spurious minimum of the Friedel potential for valences near one, as mentioned above. In fact it is probably this repulsion that favors the more close-packed structures that are actually observed. The open sc and dc structures, when compared to the close-packed structures at constant volume, have a small number of near neighbors and these near neighbors appear at relatively small values of r, as can be seen in Fig. 18. At low Z, a small value of the near neighbor distance will lead to large repulsive interactions and the preferrence of some other structure.

At larger values of Z, where the nearest neighbor vectors of the close-packed structures are approaching the adjoining maximum of the Friedel potential, the nearest neighbor distances of the open structures are near the minimum of the Friedel potential. Consequently the open structures are favored. It is interesting to note that at Z=4, the simple cubic structure is favored over the diamond cubic structure. Using the effect discussed just above, Heine and Weaire[8] suggested that the diamond cubic structure might be found to be stable at Z=4. Although the open structures are found to be more stable than the close-packed structures at Z=4, the simple cubic structure is preferred over diamond cubic, as determined by the Friedel potential. It is also of interest to note how closely the bcc curve follows the fcc and hcp curves in Fig. 4. Compared to the sc and dc structures, the bcc structure has a very clear close-packed behavior.

The computations discussed above have allowed several determinations of structure. The results are summarized in Fig. 19 along with results obtained by Blandin, Friedel and Saada.[6] The most stable structure of those considered is plotted as a function of Z. These data are also presented in Table III. In this section we compare these results with the actual structures found among the elements and in alloy systems.

The first plot in Fig. 19 represents the results of Blandin, et al.[6] Using the real space formulation of pseudopotential theory, they discussed the stability regions for the fcc and hcp structures. Specifically, they determined the regions of Z for which the fcc and hcp structures are stable against the formation of stacking faults, using the unmodified interplanar interaction.

The results which follow from the formulae of Sections IV.A and IV.B are shown in the second and third plots of Fig. 19. These results complement those of Blandin, Friedel and Saada, as can be seen by comparing the first and second plots of Fig. 19. Over the range $2.10<Z<2.20$ the fcc phase is stable against faulting for the model considered here, but is metastable with respect to the hcp phase. Similarly, the hcp phase is stable against faulting from Z=2.20 to 2.29, but is metastable with respect to the fcc structure. On the other hand, over the range $1.27<Z<1.30$ the model predicts that hcp is stable relative to the fcc structure, but unstable to faulting, while for $1.30<Z<1.36$ the fcc structure is preferred to hcp, though both are unstable with respect to formation of a fault. Since the close-packed

polytypes may be derived from the simple fcc or hcp structure through periodic faulting, polytype intrusion is likely near Z=1.30, as discussed below. At Z=1.66 and 3.53 the fcc-hcp phase boundaries coincide with the limits of stability with respect to faulting.

The results obtained from the exact summation of the Friedel potential are given in the third plot of Fig. 19, which includes the predicted range of the body centered cubic structure.

The results shown in the first three plots of Fig. 19 are complementary, and express structural tendencies which are at least roughly reflected in the periodic table for Z in the range 1 to 3. The model prefers the hcp structure when Z=1, as do the simplest monovalent metals, lithium and sodium, in their low temperature forms. At Z=2 the model shows a very slight preference for the bcc structure over an hcp structure with ideal axial ratio; the possibility of a non-ideal axial ratio was not considered. The hcp structure is clearly preferred to fcc. Empirically, the divalent metals beryllium, zinc, and cadmium are hcp; all except magnesium have axial ratios which are far from ideal. At Z=3 the model prefers the fcc structure. Among the trivalent elements, aluminum is fcc and indium is nearly fcc. Gallium has a distorted structure which was not considered.

The application of the results summarized in Fig. 18 appears to be successful in alloy systems for at least one value of Z. At Z=2.20, there is a boundary between the fcc and hcp stability regions. Corresponding to this value of Z, there are several systems with large solid solubilities that also assume a phase boundary at or near this

value of Z. The fcc phase of aluminum is stable with up to 66.5 a/o additions of zinc, and similarly the fcc phase of indium is stable with additions of up to 77 a/o magnesium.[30] Also, results from splat-cooling experiments[31] indicate that fcc or fcc-like phases are observed down to Z=2.20 in a number of systems. These experimental results for elements and alloys are in agreement with the determination of the relative stability of the fcc and hcp structures with the Friedel potential, especially in the region of Z=2 to 3.

The region of Z for which the bcc structure is preferred is $1.48<Z<2.03$. This range includes the electron-atom ratios of the beta brasses, the bcc-like Hume-Rothery alloys.[9]

Besides the fcc, hcp and bcc structures, several polytypic structures were considered in Chapter IV. In particular, results from the use of the unmodified interplanar interaction to determine the stability of the fcc, hcp, dhcp, Sm and A structures agains the formation of the other structures are shown in the second plot of Fig. 19. There is a polytype intrusion near Z=1.30. In fact, there is strong evidence[32,33] that at least the dhcp phase is found in this region of valence. At Z=2.20 the Friedel potential yields a transition between the fcc and hcp structures with no polytype intrusion. In fact, complex polytypes do not seem to intrude at or near this value of Z in alloy systems.

The considerations above relate to a model in which the valence is the only determinant of structure. Since simple metals from a particular group of the periodic chart, i.e., with a particular value of Z, display different structures, this type of determination is

bound to fail. The flexibility necessary to allow several structures to be stable at a particular value of Z is obtained by the introduction of a Friedel shift of 2δ into the Friedel potential, as can be seen from Figs. 9 and 10.

To draw clear conclusions form the modified model we would require a method for selecting an appropriate Friedel shift for a given material. The one available quantitative suggestion,[21,34] that the phase factor be computed from the phase shifts on scattering from the pseudopotential, has been criticized on theoretical grounds by Heine and Weaire.[35] We computed phase factors from the phase shifts on scattering from several suggested model potentials and found, in agreement with Seeger,[20] that the resulting values of 2δ are so large that they destroy the reasonable agreement between the simple structural model and empirical trends in structure. Reasonable agreement can only be maintained if one accepts the conclusion of Heine and Weaire[35] that 2δ is small.

Leaving aside the computation of the phase factor, the accuracy of the model may be improved if 2δ is allowed to assume values of magnitude $\pi/4$ or less. Reference to Fig. 9 shows that at Z=3 this range of 2δ permits the fcc and hcp structures, which are empirically observed, but does not permit the bcc structure, which is not observed. At Z=2 all three structures, hcp, bcc, and fcc, occur over a small range of 2δ; all are, in fact, found in the divalent metals. At Z=1 the hcp and bcc structures occur with moderate phase factor; these are the structures found in the monovalent alkali metals. Reference to

Fig. 10 shows that polytypic phases may be stabilized by a small phase factor when $1.25<Z<1.60$ and when $3.00<Z<3.60$. These are the ranges of electron-atom ratio over which the close-packed polytypes are commonly found.[11]

The second modification to the Friedel potential that we consider is actually a class of modifications to the interplanar interaction. The value of $\Delta\phi(2d)$ is adjusted to find ranges of Z where the complex polytypes, dhcp, Sm and A, might occur in the case that $\Delta\phi(2d)$ is not given correctly by the expression of Blandin, Friedel and Saada, $\Delta\phi^{BFS}(2d)$. More distant interactions are still assumed to be given by Eq. (III.21).

The last two plots in Fig. 19 show the regions where the complex polytypes might occur according to the modifications discussed in Section IV.D. In both of these plots, polytype intrusions occur at Z=1.30, as was the case for the results from the unmodified interplanar interaction. It is interesting to note that the A structure appears in the last plot only and there the A structure is stable only in relatively small regions of Z. Experimentally, the A structure is rarely found.

The last plot in Fig. 19, which shows where polytypes might occur if $\varepsilon_{fcc}=\varepsilon_{hcp}$, gives results close to those listed by Havinga, et al.[11] who used a criterion even more general than the criteria described above to discuss polytypes. These authors did not use complete summations, Eq. (IV.2), in their determiantion of polytype stability, but inserted a factor which damped the interplanar interaction at large distances.

In contrast, the technique used in this paper treats the long range part of the Friedel potential explicitly. However, we note that there are experimentally observed polytypes listed by Havinga, et al. which fall outside the stability zones found in their paper and in Fig. 19.

B. Criteria for Stability

The determination of the crystal lattice with the lowest structural energy, as discussed in the previous section, is only one of a number of ways of viewing the stability of lattices. The calculations of previous chapters allow several other approaches. Moreover, since results from the Friedel potential depend on the valence associated with the metallic alloy, and only the valence, the different criteria for stability that emerge can be studied for the whole family of potentials generated by allowing the valence to vary. In this section, the magnitude of the physical quantities involved will not be of so much concern as the determination of whether or not the quantities satisfy the various stability criteria.

The interpretation of the phenomena predicted by a microscopic model for metallic bonding in terms of the details of the interatomic potential used in the model, if an interatomic potential is indeed used, is necessary for a complete understanding of the model. On the other hand, this task is complicated since any ion is interacting with all other ions in the solid which is being modelled, and these ions are situated in all different directions and at all different distances

from the original ion. The interplanar interaction and its application to various shear-like phenomena was developed to allow a simplification of this interpretive problem. Although shear deformations cannot be used to characterize many processes in metals, a shear is the simplest volume conserving deformation, so while the restriction to shear deformations below is fairly severe, this direction is probably the place to start an interpretation of the consequences of the model in terms of the interatomic potential used above.

Stability against phase transformation and against stacking fault formation have already been discussed in the previous section. If the axial ratio is assumed to be ideal, then only interactions between second nearest neighbor planes enter into the consideration of stability using these two criteria. As noted in the previous section, the determination of stability against phase transformation by finding the lattice with the minimum structural energy ensures that only one structure will meet the criterion; this was not the case for the formation of stacking faults. Using this latter criterion and the two criteria discussed below, more than one structure can be stable at some values of Z. These criteria are for mechanical stability, and in terms of the discussion of phase and mechanical stability in the introduction, only metastability can be treated with mechanical stability criteria.

Two other mechanical stability criteria for stability emerge from Chapter IV. First the requirement that all phonon frequencies be real must be satisfied. A special case of this criterion is that

$(C_{11} - C_{12} + C_{44})/3 > 0$ for fcc lattices and $C_{66} > 0$ for hcp lattices. These relations are implied by the Born stability criteria[22] and comprise the second new means by which the stability of a lattice can be tested. In Fig. 20 are plotted stability zones for fcc and hcp lattices using all four criteria. Clearly, the above criteria on the elastic constants are not sufficient to ensure $\omega > 0$ for all values of the phonon wave vector, since there are regions of Z in the last plot of Fig. 20 which show stability while the corresponding transverse phonon modes indicate instability.

At small values of Z, we can also see that neither the fcc or hcp structures are metastable. Evidently some other structure is more stable than those indicated in second plot of Fig. 20. This fact has already been verified for Z equal to 1.3.

Still assuming ideal axial ratios, there appears a significant distinction between the stability criteria based on stability against phase transformation and stability against stacking fault formation on the one hand, and the criteria based on elastic constants and phonon frequencies on the other. For the shear across a ⟨111⟩ plane in an fcc crystal, only interactions between second nearest neighbor planes enter in the first case, while in the second case, near neighbor plane interactions enter. Whether this phenomenon occurs for other types of deformation has not been investigated, but it has significance for the study of polytype stability.

It might be expected that, as a structure becomes unstable against the formation of a phase which is the polytype of the original phase, the corresponding elastic shear modulus and transverse phonon branch might show some anomaly. Such polytypic transformations have been observed in magnesium and the rare earth elements. As it appears from the above considerations, such anomalies will be small or non-existent simply because polytype stability is determined by a different combination of interactions than the combination of interactions which determine the phonon dispersion relative in the ⟨111⟩ direction.

C. Conclusion

The model of a metal adapted above has yielded some insight into the relationships between different aspects of lattice stability. Below, we return to some question raised in the introduction and then indicate the direction further work might take.

Two questions have underlaid the present work: 1) What is the range of bonding in metals, i.e., how rapidly do the strengths of bonding functions decrease in metallic alloys, and 2) are phase transformations manifested in the behavior of the macroscopic parameters characterizing the phases, and does such a manifestation yield information about how the transformation proceeds?

The first question is an old one and remains controversial. As discussed above, the odd dependence (or independence) of contributions to elastic constants on interplanar separation is an example of some of the paradoxes which arise in attempting to find an answer. To some

extent, the question is not very important in that many quantities--phonon spectra, elastic constants, etc.--can be obtained from interatomic potentials vastly different from the type used above. It is in second order effects that the range of bonding may become important. It is in the temperature and pressure dependence of elastic constants, stacking fault energies and more subtle effects that the range of bonding may enter as an important quantity.

The answer to the remaining question regarding phase transformations is of great practical importance. Although the questions have not been addressed directly in the development above, they can be discussed qualitatively using some general thermodynamic ideas. Phase transformations can be categorized in many ways, but one of the most useful is use of the distinction between reconstructive and non-reconstructive[36] transformations. In the former, the unit cell of the two phases (or structures) differ radically, i.e., relatively large displacements of atoms are required by the transformation. In the latter case, small displacements are usually encountered. It has been found that optical and elastic constants do indeed show anomalous behavior near transition temperatures when displacements are reasonably small. This area of research has received much attention recently.

However, it is the former area which is perhaps of more importance to metallurgists--included are many allotropic phase transformations. It is perhaps a pessimistic stance, but it seems unlikely that simply because the free energies of two modifications of a metallic alloy are nearly equal, other parameters will show any anomalous behavior. The

reason for this lies in the idea that thermodynamically, the region of phase space sampled by one phase is too far removed from the phase space sampled by the other phase for the first phase to manifest behavior connected to the incipience of the second phase. In some sense, the equality of the free energies may be considered as accidental so that the phase transformation cannot be viewed as the "freezing in" of a phonon or the results of some other mechanism. That such transformations can be analyzed in terms of so-called soft modes seems unlikely.

We have omitted any consideration of temperature or pressure effects in the preceding development. Some temperature effects can be included directly in the interionic potential. These include 1) the effect of thermal excitation of the electrons[37] which reduces the sharpness of the electron energy distribution function which in turn yields the Friedel oscillations, 2) the vibrations of the ions which does not allow a unique assignment of interionic distances, and 3) mean free path effects. All of these mechanism tend to weaken the Friedel potential, or any other interionic potential, as the temperature is increased.

Two problems arise if temperature effects are included directly in an interatomic potential. First of all, some temperature effects will be omitted in this approach because only part of the Gibbs free energy is being calculated to start with. The term - TS in the Gibbs free energy is obviously of importance to the stability of alloys at finite temperature, and the entropic effects must be considered in

addition to what has been done above or in most applications of pseudopotential theory, for that matter. Secondly, the contribution of excited phonons to the free energy is difficult to separate from electronic effects. Nonetheless, some temperature effects have already been incorporated in interatomic potentials derived from pseudopotential theory.[38]

Crystal lattices under finite stress have not been considered at all above. This field, which includes anharmonic effects, theoretical strengths of crystals, and the effect of finite distortions, is of great importance.

ACKNOWLEDGEMENTS

This work was done under the auspices of the United States Atomic Energy Commission.

My sincere thanks to the members of the Department of Materials Science and Engineering at Berkeley, the able occupants of notorious Building 62 at Lawrence Berkeley Laboratory, and my other friends for their encouragement, and to Bill Morris, Walt Harrison and Leo Brewer for having enough energy to plow through the preceding pages.

My two sisty uglers, Marilee and Carolyn, ungrudgingly provided the space for their brother to take care of his business. My parents, Derwood and Mary Helen, provided two more ingredients required for completion of this tome--requited love and unrequited money. I thank my family, the worthy object of my pride and affection.

Finally, there is no better way than to say "Cherchez la femme."

APPENDIX A

Derivation of the Inverse Fourier Transform of the Friedel Potential

Care must be taken in the evaluation of the Fourier transforms related to the partial summations of Chapter III. The convention that will be used for f(x) and the Fourier transform of f(x), g(y), is

$$f(x) \int_{-\infty}^{\infty} dy \exp ixy\, g(y)$$
$$g(y) = \frac{1}{2\pi} \int_{-\infty}^{\infty} dx \exp -ixy\, f(x) \; . \tag{A.1}$$

Most of the transforms that are needed can be found in Lighthill[39] and are expressed there following a slightly different convention:

$$f(x) = \int_{-\infty}^{\infty} dy \exp(2\pi ixy) g'(y)$$
$$g'(y) = \int_{-\infty}^{\infty} dx \exp -(2\pi ixy) f(x) \tag{A.2}$$

where g'(y) designates the Fourier transform of f(x). The two Fourier transforms are related by

$$g(y) = \frac{1}{2\pi} g'(y/2\pi). \tag{A.3}$$

It is desired to find w(k), the inverse Fourier transform of the Friedel potential, i.e., the function whose Fourier transform is the Friedel potential:

$$w(k) = \frac{1}{2\Omega} \int d^3r \exp i\vec{k}\cdot\vec{r} \; \frac{\cos 2k_F r}{(2k_F r)^3} \tag{A.4}$$

where the insertion of the factor of $(1/2\Omega)$ ensures consistency with Eq. (III.3). If use is made of spherical coordinates with the z axis parallel to $\vec{k}$, the angular integrals may be performed immediately:

$$w(k) = \frac{2\pi}{2\Omega(2k_F)^3 ki} \int_0^\infty dr \; \frac{\cos\, 2k_F r}{r^2} (\exp ikr - \exp -ikr) = \tag{A.5}$$

$$\frac{\pi}{2\Omega(2k_F)^3 ki} \int_0^\infty dr \; \frac{1}{r^2} \left\{ \begin{matrix} \exp i(k+2k_F)r + \exp i(k-2k_F)r \\ -\exp i(-k+2k_F)r - \exp i(-k-2k_F)r \end{matrix} \right\}$$

Now the appropriate Fourier transform of $1/x^2$ can be found in Lighthill:[39]

$$\frac{1}{2\pi} \int_0^\infty dx \; \frac{1}{x^2} \; \exp -ikx = \frac{1}{2\pi} \int_{-\infty}^\infty dx \; \frac{1}{x^2} \; \exp -ikx \; H(x) \tag{A.6}$$

$$= \frac{ik}{2\pi} \left(\frac{\pi i}{2} \operatorname{sgn}(k) + \ln|k/2\pi| + C\right)$$

where H(x) is the Heaviside function, $\operatorname{sgn}(k) = |k|/k$, and C is an arbitrary constant. C arises from the indeterminancy of $1/x^2$ at x=0; as defined as a generalized function, $1/x^2$ contains an arbitrary admixture of delta functions. The value of C in fact will depend

upon the units used for k and will be dropped here because the Fourier transforms of w(k) developed elsewhere simply render C into a delta function at the origin again. In other words w(k) will never be used directly, and the same applies to the factor of $(1/2\pi)$ that appears in the logarithmic term of Eq. (A.6). Application of Eq. (A.6) to Eq. (A.5) yields

$$w(k) = \frac{2\pi}{2\Omega k(2k_F)^3}\left[(k+2k_F)\ln|k+2k_F| + (k-2k_F)\ln|k-2k_F|\right] \qquad (A.7)$$

It will be noted that as $k\to\infty$, $w\to\infty$ logarithmically. Also worth noting is that if Eq. (III.2) is carried to the limit $k\to\infty$, a singularity identical to Eq. (A.7) appears upon expansion of the exponential integrals in the reciprocal space sum. This is expected.

APPENDIX B.

The Asymptotic Form of $\phi(g_\perp, z)$

The function $\psi(g_\perp, z)$ is given by the integral

$$\psi(g_\perp, z) = \frac{2\Omega}{2\pi A} \int_{-\infty}^{\infty} dk_\parallel \exp -ik_\parallel z \quad w(\sqrt{k_\parallel^2 + g_\perp^2}) \tag{B.1}$$

where

$$w(k) = \frac{2\pi}{(2\Omega)k(2k_F)^3} [(k+2k_F)\ln|k+2k_F| + (k-2k_F)\ln|k-2k_F|] . \tag{B.2}$$

As per Lighthill,[39] only the singular part of Eq. (B.2) will contribute to the asymptotic form of $\phi(g_\perp, z)$. Since $\sqrt{k_\parallel^2 + g_\perp^2} \geq 0$, only the term $(k-2k_F)\ln|k-2k_F|$ will contribute and only if $2k_F > g_\perp$. Here, $2k_F$ will be restricted to lie between the first and second non-zero reciprocal lattice vectors. In this case, the singularity occurs at $k_\parallel$ determined by

$$\sqrt{k_\parallel^2 + g_\perp^2} - 2k_F = 0 \tag{B.3}$$

or at

$$k_\parallel = \pm \sqrt{4k_F^2 - g_\perp^2} \equiv \pm 2k_o$$

where k_o is defined in order to simplify the equations below. Now the nature of the singularity of $w(k)$ at $\pm 2k_o$ must be found. For $|k_\parallel - 2k_o|$ small, it is easily shown that

$$\sqrt{k_\parallel^2 + g_\perp^2} - 2k_F = (k_\parallel - 2k_o)\frac{k_o}{k_F} \tag{B.4}$$

Substitution into w(k) yields a singularity of the form

$$\frac{2\pi}{(2\Omega)\left(\sqrt{k_{\parallel}^{\,2}+g_{\perp}^{\,2}}\right)(2k_F)^3}\left(\sqrt{k_{\parallel}^{\,2}+g_{\perp}^{\,2}}-2k_F\right)\ln\left|\sqrt{k_{\parallel}^{\,2}+g_{\perp}^{\,2}}-2k_F\right|$$

$$= \frac{2\pi}{(2\Omega)(2k_F)^4}\,\frac{k_o}{k_F}\,(k_{\parallel}-2k_o)\,\ln\left|(k_{\parallel}-2k_o)\,\frac{k_o}{k_F}\right| \qquad (B.5)$$

$$\sim \frac{2\pi}{(2\Omega)(2k_F)^4}\,\frac{k_o}{k_F}\,(k_{\parallel}-2k_o)\,\ln\left|k_{\parallel}-2k_o\right|$$

near $k_{\parallel} = +2k_o$, where the non-singular part which behaves like $\ln|k_o/k_F|$ has been dropped. Similarly, at $k_{\parallel} = -2k_o$, there is a singularity of the form

$$\frac{-2\pi}{(2\Omega)(2k_F)^4}\,\frac{k_o}{k_F}\,(k_{\parallel}+2k_o)\,\ln\left|k_{\parallel}+2k_o\right| \qquad (B.6)$$

Substitution of the singularities (B.5) and (B.6) into (B.1) yields an asymptotic form of

$$\psi(g_{\perp},z) = -\frac{\pi\,k_o}{2A\,k_F^{\,3}}\,\frac{\sin 2k_o z}{(2k_F z)^2} \qquad (B.7)$$

APPENDIX C

Lattice Vectors

Direct and reciprocal lattice vectors for three dimensional lattices can be found in a number of places[1,40] or can be determined directly. The characteristic lattice vectors for a planar hexagonal lattice enter so frequently in the text that they will be determined below. Vectors will be designated with an arrow, e.g., $\vec{b}$, and unit vectors will be shown with a caret, e.g., $\hat{b}$.

Using the conventions of Barrett and Massalski[41] and the usual dimensionless unit vectors for a Cartesian coordinate system, the unit vectors for the hexagonal planar lattice are just

$$\hat{a}_1 = \hat{x}$$

$$\hat{a}_2 = -\frac{\hat{x}}{z} + \frac{\sqrt{3}}{2}\,\hat{y} \qquad \text{(C.1)}$$

The translation vectors for the planar hexagonal lattice are given by

$$\vec{a}_1 = a\,\hat{a}_1$$

and (C.2)

$$\vec{a}_2 = a\,\hat{a}_2$$

The condition[3] to be satisfied by the reciprocal lattice vectors, designated $\vec{g}_{l1}$ and $\vec{g}_{l2}$, are that

$$\begin{aligned} \vec{g}_{\perp 1}\cdot\vec{a}_1 &= 2\pi & \vec{g}_{\perp 1}\cdot\vec{a}_2 &= 0 \\ \vec{g}_{\perp 2}\cdot\vec{a}_1 &= 0 & \vec{g}_{\perp 2}\cdot\vec{a}_2 &= 2\pi \end{aligned} \tag{C.3}$$

This set of equations lead to

$$\begin{aligned} \vec{g}_{\perp 1} &= \frac{8\pi}{3a}\left(\hat{a}_1 + \frac{\hat{a}_2}{2}\right) = \frac{4\pi}{\sqrt{3}a}\left(\frac{\sqrt{3}}{2}\hat{x} + \frac{1}{2}\hat{y}\right) \\ \vec{g}_{\perp 2} &= \frac{8\pi}{3a}\left(\frac{\hat{a}_1}{2} + \hat{a}_2\right) = \frac{4\pi}{\sqrt{3}a}\hat{y} \end{aligned} \tag{C.4}$$

with

$$|\vec{g}_{\perp 1}| = |\vec{g}_{\perp 2}| = \frac{4\pi}{\sqrt{3}a} \quad .$$

With these reciprocal lattice vectors, the rest of the reciprocal lattice can be generated.

The points of the reciprocal lattice generated by the vectors from Eq. (C.4) will be labelled according to their distance from the origin of the lattice. The quantity $\vec{g}_{\perp}^{\,o}$ will designate the origin, $\vec{g}_{\perp}^{\,1}$ will designate the first near neighbor lattice positions and so forth. The first four such sets of reciprocal lattice vectors are given in terms of $\hat{a}_1$ and $\hat{a}_2$ as follows:

$\vec{g}_{\perp}^{o}$: 0

$\vec{g}_{\perp}^{1}$: $\frac{8\pi}{3a}(1,\frac{1}{2})$ $\frac{8\pi}{3a}(\frac{1}{2},1)$

$\frac{8\pi}{3a}(-1,-\frac{1}{2})$ $\frac{8\pi}{3a}(-\frac{1}{2},-1)$

$\frac{8\pi}{3a}(\frac{1}{2},-\frac{1}{2})$ $\frac{8\pi}{3a}(-\frac{1}{2},\frac{1}{2})$

$\vec{g}_{\perp}^{2}$: $\frac{8\pi}{3a}(\frac{3}{2},\frac{3}{2})$ $\frac{8\pi}{3a}(0,\frac{3}{2})$

$\frac{8\pi}{3a}(-\frac{3}{2},0)$ $\frac{8\pi}{3a}(-\frac{3}{2},-\frac{3}{2})$

$\frac{8\pi}{3a}(0,-\frac{3}{2})$ $\frac{8\pi}{3a}(\frac{3}{2},0)$

$\vec{g}_{\perp}^{3}$: $\frac{8\pi}{3a}(2,1)$ $\frac{8\pi}{3a}(1,2)$

$\frac{8\pi}{3a}(-2,-1)$ $\frac{8\pi}{3a}(-1,-2)$

$\frac{8\pi}{3a}(1,-1)$ $\frac{8\pi}{3a}(-1,1)$

APPENDIX D

Summation Formulae

It is required that a method of evaluating sums such as

$$\sum_{m=1}^{\infty} \Delta\phi(6m-3) \propto \sum_{m=1}^{\infty} \frac{\sin(6m-3)\theta}{(6m-3)^2}$$

be obtained. To do this, we fix j and k and show that

$$F(j,k,\theta) \equiv \sum_{n=1}^{\infty} \exp i[(jn-k)\theta]\, f(jn-k)$$

$$= \frac{1}{j} \sum_{\ell=0}^{j-1} \exp \frac{2\pi i k \ell}{j} \sum_{n=1}^{\infty} \exp i[n(\theta + \frac{\ell 2\pi}{j})]f(n)$$

where f(n) is any function of the i.e. $\sum_{n=1}^{\infty} f(n)$ must converge absolutely natural numbers such that $F(j,k,\theta)$ exists. Notice that the expression in braces above is in general easier to evaluate than $F(j,k,\theta)$ itself, and it may often be given in an analytic form.

We have

$$F(j,k,\theta) = \sum_{n=1}^{\infty} \exp i[(jn-k)\theta]\, f(jn-k)$$

$$= \frac{1}{j} \sum_{n=1}^{\infty} \sum_{\ell=0}^{j-1} \exp i[(jn-k)\theta + \frac{jn\ell 2\pi}{j} - \frac{k\ell 2\pi}{j} + \frac{k\ell 2\pi}{j}]f(jn-k)$$

$$= \frac{1}{j} \sum_{n=1}^{\infty} \sum_{\ell=0}^{j-1} \exp i[(jn-k)(\theta + \frac{\ell 2\pi}{j})]\exp \frac{ik\ell 2\pi}{j} f(jn-k) \quad .$$

Now we replace jn-k by n' and sum over n' from 1 to ∞. This does not change $F(j,k,\theta)$ since all terms of the new sum vanish except those for which n'=jn-k for some positive integral value of n. If this can be established, the above assertion holds true, i.e.,

$$F(j,k,\theta) = \frac{1}{j} \sum_{n'=1}^{\infty} \sum_{\ell=0}^{j-1} \exp\, i(n'(\theta + \frac{2\pi\ell}{j})) \exp \frac{2\pi i k \ell}{j} f(n')$$

For given n', j and k, suppose there is no n such that n'=jn-k. We show

$$F' = \sum_{\ell=0}^{j-1} \exp\, in'(\theta + \frac{2\pi\ell}{j}) \exp \frac{ik\ell 2\pi}{j} = 0$$

There must be some p such that $n' + p = jn-k$ for some n, with $0<p<j$:

$$F' = \sum_{\ell=0}^{j-1} \exp\, i(jn-k-p)(\theta + \frac{2\pi\ell}{j}) \exp \frac{ik\ell 2\pi}{j}$$

$$= \exp\, i(jn-k-p)\theta \sum_{\ell=0}^{j-1} \exp\, i(\frac{2\pi jn\ell}{j} - \frac{2\pi k\ell}{j} - \frac{2\pi p\ell}{j} + \frac{k\ell 2\pi}{j})$$

$$= \exp\, i(jn-k-p)\theta \sum_{\ell=0}^{j-1} \exp - \frac{2\pi i p\ell}{j}$$

and, indeed, the above sum is zero. An example of the way this result simplifies an expression is given below.

$$\sum_{n=1}^{\infty} \frac{\sin(jn-k)\theta}{(jn-k)^2} = \text{Im} \sum_{n=1}^{\infty} \frac{\exp i[(jn-k)\theta]}{(jn-k)^2}$$

$$= \text{Im} \frac{1}{j} \sum_{\ell=0}^{j-1} \exp \frac{ik\ell 2\pi}{j} \sum_{n=1}^{\infty} \frac{\exp i[n(\theta + 2\pi\ell/j)]}{n^2}$$

$$= \text{Im} \frac{1}{j} \sum_{\ell=0}^{j-1} \exp \frac{2\pi ik\ell}{j} (\beta_2(\theta + \frac{\ell 2\pi}{j}) + i\alpha_2(\theta + \frac{2\pi\ell}{j}))$$

$$= \frac{1}{j} \sum_{\ell=0}^{j-1} \sin \frac{2\pi k\ell}{j} \beta_2(\theta + \frac{2\pi\ell}{j}) + \cos \frac{2\pi k\ell}{j} \alpha_2(\theta + \frac{2\pi\ell}{j})$$

The functions α_2 and β_2 are simple forms given by Blandin, et al. Also used is

$$\sum_{n=1}^{\infty} \frac{\cos(jn-k)\theta}{(jn-k)^2} = \frac{1}{j} \sum_{\ell=0}^{j-1} \cos \frac{2\pi k\ell}{j} \beta_2 \frac{(\theta + 2\pi\ell)}{j} - \sin \frac{2\pi k\ell}{j} \alpha_2 \frac{(\theta + 2\pi\ell)}{j} .$$

REFERENCES

1. W. A. Harrison, Pseudopotentials in the Theory of Metals, Benjamin, N.Y. (1966).

2. M. H. Cohen, Metallic Solid Solutions, edited by J. Friedel and A. Guinier, p. XI-1, Benjamin, N.Y. (1963).

3. C. Kittel, Introduction to Solid State Physics, 3rd ed., Wiley, N.Y. (1966).

4. J. Friedel, Trans. Met. Soc. AIME 230, 616 (1964).

5. A. J. E. Foreman and W. M. Lomer, Proc. Phys. Soc. (London) B70, 1143 (1957).

6. A. P. Blandin, Phase Stability in Metals and Alloys, edited by P.S. Rudman, J. Stringer, and R. I. Jaffer, p. 115, McGraw Hill, N.Y. (1967). A. Blandin, J. Friedel and G. Saada, Proceedings of the Toulouse Conference on Dislocations, J. Phys. C3, 128 (1966).

7. C. W. Krause and J. W. Morris, Jr., Acta Met. 22, 767 (1974).

8. V. Heine and D. Weaire, Solid State Physics, Vol. 24, edited by H. Ehrenreich, F. Seitz, and D. Turnbull, p. 249, Academic, N.Y. (1970).

9. R. W. Shaw, Jr., Ph.D. Thesis, Standford University (1968). W. Harrison, Physical Chemistry, an Advanced Treatise, Vol. 5, edited by H. Eyring, p. 525, Academic, N.Y. (1970).

10. C. H. Hodges, Acta Met. 15, 1787 (1967).

11. E. E. Havinga, J. H. N. van Vucht, and K. H. J. Buschow, Philips Res. Repts. 24, 407 (1969).

12. W. Hume-Rothery, R. E. Smallman, and C. W. Haworth, The Structure of Metals and Alloys, Chaucer, London (1969).

13. L. Brewer, High-Strength Materials, edited by V. Zackay, p. 12, Wiley, N.Y. (1965).

14. P. Epstein, Math. Ann. 56, 615 (1903); 63, 205 (1907).

15. C. S. G. Cousins, J. Phys. F 4, 1 (1974).

16. J. Rabier and J. Grilhe, J. Phys. Chem. Solids 34, 1031 (1973).

17. B. R. A. Nijboer and F. W. DeWette, Physica 23, 309 (1957).

18. J. Friedel, Advan. Phys. 3, 446 (1954).

19. J. Friedel, Phase Stability in Metals and Alloys, edited by P. S. Rudman, J. Stringer, and R. I. Jaffee, p. 236, McGraw-Hill, N.Y. (1967).

20. A. Seeger, Phase Stability in Metals and Alloys, edited by P. S. Rudman, J. Stringer, and R. I. Jaffee, p. 249, McGraw-Hill, N.Y. (1967).

21. W. A. Harrison, Phys. Rev. B7, 2408 (1973).

22. M. Born and K. Huang, Dynamical Theory of Crystal Lattices, Oxford (1968).

23. S. H. Koenig, Phys. Rev. 135, A1693 (1964).

24. P. K. Iyengar, G. Venkataraman, P. R. Vijayaraghavan and A. P. Roy, Neutron Inelastic Scattering, Vol. I, p. 153, IAEA, Vienna (1965).

25. R. Stedman and G. Nilsson, Phys. Rev. 145, 492 (1966).

26. M. Appapillai and A. R. Williams, J. Phys. F 3, 759 (1973).

27. P. C. J. Gallagher, Met. Trans. A.I.M.E. 1, 2429 (1970).

28. E. A. Harrison, Acta Met. 20, 1387 (1972).

29. C. S. G. Cousins, J. Phys. F 4, 1 (1974).

30. M. Hansen, Constitution of Binary Alloys, McGraw-Hill, N.Y. (1958).

31. B. C. Giessen, Advances in X-ray Analysis, Vol. 12, edited by C. S. Barrett, J. B. Newkirk, and G. R. Mallett, p. 23, Plenum, N.Y. (1969).

32. C. J. Cooke and W. Hume-Rothery, J. Less Com. Met. 10, 42 (1966).

33. S. E. R. Hiscocks and W. Hume-Rothery, Proc. R. Soc. 282, 318 (1964).

34. K. Bennemann, Phys. Rev. 133, 1045 (1964); 139, 482 (1965).

35. Ref. 8, p. 346.

36. J. F. Scott, Revs. of Mod. Phys. 46, 83 (1974).

37. M. F. Merriam, private communication.

38. N. W. Ashcroft, Interationic Potentials and Simulation of Lattice Defects, edited by P. C. Gehlen, J. R. Beeler, Jr., and R. I. Jaffee, p. 91, Plenum, N.Y. (1972).

39. M. J. Lighthill, Introduction to Fourier Analysis and Generalized Functions, Cambridge (1964).

40. D. C. Wallace, Thermodynamics of Crystals, Wiley, N.Y. (1972).

41. C. S. Barrett and T. B. Massalski, Structure of Metals, 3rd ed., McGraw-Hill, N.Y. (1966).

Table I. Free electron and pseudopotential parameters taken from Appapillai and Williams.[26] Values of V_o were calculated using Eq. (II.4) of the text. Except for the last column, atomic units are used throughout the table.

Element	Z	k_F	E_F	w_{2k_F}	V_o	V_o(eV)
Li	1	.5890	.1735	.04604	.345	9.40
Na	1	.4882	.1192	.00467	.00517	.141
K	1	.3947	.0779	.00142	.00073	.0199
Rb	1	.3693	.0682	-.00187	.00144	.0394
Cs	1	.3412	.0582	-.00145	.00102	.0278
Be	2	1.0287	.5291	.18280	7.14	194.
Mg	2	.7242	.2622	.02456	.260	7.08
Ca	2	.5865	.1720	.00960	.0606	1.65
Sr	2	.5380	.1447	.01959	.300	8.16
Ba	2	.5188	.1346	-.00012	.00001	.00032
Zn	2	.8342	.3479	.02626	.224	6.10
Cd	2	.7432	.2762	.01844	.139	3.79
Hg	2	.7213	.2601	.00310	.00417	.114
Al	3	.9276	.4302	.04197	1.04	28.3
Ga	3	.8776	.3851	.03053	.616	16.8
In	3	.7972	.3178	.03165	.802	21.8
Tl	3	.7738	.2994	.03881	1.28	34.8
Si	4	.9590	.4598	.03283	1.06	28.8
Ge	4	.9206	.4236	.02928	.915	24.9
Sn	4	.8674	.3762	.02941	1.04	28.3
Sn(G)	4	.8007	.3206	.01507	.320	8.72
Pb	4	.8350	.3486	.03140	1.28	34.8

Table II. Stacking Characteristics of Polytypes

Structure	Stacking	Symmetry	
fcc	ABCABC	kkkk	3R
hcp	ABABAB	hhhh	2H
dhcp	ABACABAC	hkhk	4H
Sm	ABABCBCAC	hhkhhk	9R
A	ABCBAC	kkhkkh	6H

Table III. The regions of Z for which structures are stable against the formation of the other structures considered.

Exact Summation: fcc, hcp and bcc		Interplanar Interaction: fcc, hcp, dhcp, Sm and A	
Z	Structure	Z	Structure
1.00-1.28	hcp	1.00-1.24	hcp
1.28-1.48	fcc	1.24-1.26	Sm
1.48-2.03	bcc	1.26-1.34	dhcp
2.03-2.21	hcp	1.34-1.66	fcc
2.21-3.53	fcc	1.66-2.20	hcp
3.53-4.00	hcp	2.20-3.53	fcc
		3.53-4.00	hcp

$\Delta\phi(2d) = 0$: fcc, hcp, dhcp, Sm and A		$\varepsilon_{fcc} = \varepsilon_{hcp}$: fcc, hcp, dhcp, Sm and A	
Z	Structure	Z	Structure
1.00-1.21	fcc	1.00-1.17	fcc-hcp
1.21-1.26	Sm	1.17-1.20	Sm
1.26-1.35	dhcp	1.20-1.23	A
1.35-1.37	hcp	1.23-1.25	Sm
1.37-1.66	fcc	1.25-1.36	dhcp
1.66-1.84	hcp	1.36-1.53	fcc-hcp
1.84-1.87	dhcp	1.53-1.66	Sm
1.87-2.08	Sm	1.66-1.95	dhcp
2.08-2.56	fcc	1.95-2.11	Sm
2.56-2.68	dhcp	2.11-2.52	fcc-hcp
2.68-2.95	hcp	2.52-2.92	dhcp
2.95-3.53	Sm	2.92-2.96	A
3.53-3.67	hcp	2.96-3.53	Sm
3.67-4.00	fcc	3.53-4.00	fcc-hcp

Table IV. Stacking Sequences Induced by Planar Faults.

Face-centered cubic structure:	
Intrinsic fault	ABCBCABC kkhhkkkk
Extrinsic fault	ABCBABCABC kkhkhkkkkk
Twin	ABCBACBA kkhkkkkk
Hexagonal close-packed structure:	
Intrinsic fault	BABCACA hhkkhhh
Extrinsic fault	BABCABAB hhkkkhhh
Twin	BABCBCB hhkhhhh

FIGURE CAPTIONS

Fig. 1. Illustration of notation used in the derivation of the interplanar interaction.

Fig. 2. Illustration of notation used in the generalized interplanar interaction.

Fig. 3. Illustration of notation used in the derivation of the interlinear interaction.

Fig. 4. Dimensionless energies ε_{fcc}, ε_{hcp} and ε_{bcc} obtained from summation of the Friedel potential.

Fig. 5. Results for the dimensionless relative energies, $\varepsilon_{hcp}-\varepsilon_{fcc}$ and $\varepsilon_{bcc}-\varepsilon_{fcc}$, as determined by exact summation of the reduced Friedel potential as a function of Z.

Fig. 6. Dimensionless energies ε_{fcc}, ε_{sc} and ε_{dc} obtained from summation of the Friedel potential.

Fig. 7. Results for the dimensionless energies of the polytypic structure hcp, dhcp, Sm and A relative to the fcc structure as determined from the BFS interplanar interaction as a function of Z. See Table II for the description of the packing of these structures. The region $Z < 1.14$ has been omitted for clarity.

Fig. 8. Comparison of the dimensionless energy difference $\varepsilon_{hcp}-\varepsilon_{fcc}$ as determined with the exact summation and the interplanar interaction as of function of Z. The results from the BFS interplanar interaction are a good approximation to those from the exact summation, except near $Z = 1.14$.

Fig. 9. Results from the determination of the most stable structure among fcc, hcp and bcc from the exact summation of the Friedel potential as a function of Z and a phase factor, 2δ. Legend for identification of structures as in Fig. 19.

Fig. 10. Results from the determination of the most stable structure from among fcc, hcp, dhcp, Sm and A using the interplanar interaction as a function of Z and 2δ. Legend for identification of polytypic structures as in Fig. 18.

Fig. 11. Phonon dispersion relations ($\langle 111 \rangle$ T) as calculated with the interplanar stiffness constants for the fcc structure for various values of the valence.

Fig. 12. Phonon dispersion relations ($\langle 001 \rangle$ T) in the extended zone scheme as calculated with the interplanar stiffness constants for the hcp structure for various values of the valence.

Fig. 13. Phonon dispersion curves for Mg ($\langle 001 \rangle$ T): points are experimental data; curve is the calculated result.

Fig. 14. Phonon dispersion curves for Al ($\langle 111 \rangle$ T): dashed line indicates experimental points; solid curve is the calculated result.

Fig. 15. Dimensionless stacking fault energy of hcp structure, at Z=2 as calculated in Section VI.A.

Fig. 16. The relationship between bct and fcc unit cells.

Fig. 17. Dimensionless energy as a function of c/a for bct structure at selected values of the valence. Note change of scale between to parts of the figure.

Fig. 18. The Friedel potential for Z=1, 2,3 and 4.

Fig. 19. Values of Z for which various structures are stable: A) stability against faulting of fcc and hcp after Blandin, Friedel, and Saada, B) relative stability of polytypes from interplanar interaction, C) relative stability of fcc, hcp and bcc from exact summation, D and E) polytype stability using the modified interplanar interactions given in Eqs. (IV.8) and (IV.9), respectively.

Fig. 20. Values of Z for which various stability criteria are satisfied for the fcc and hcp structures, as evaluated with the interplanar interaction: A) stability against faulting after Blandin, Friedel and Saada, B) relative phase stability; C) real phonon frequencies, and D) positive elastic constants.

Fig. 21. Direct and reciprocal lattice vectors for hexagonal close-packed plane.

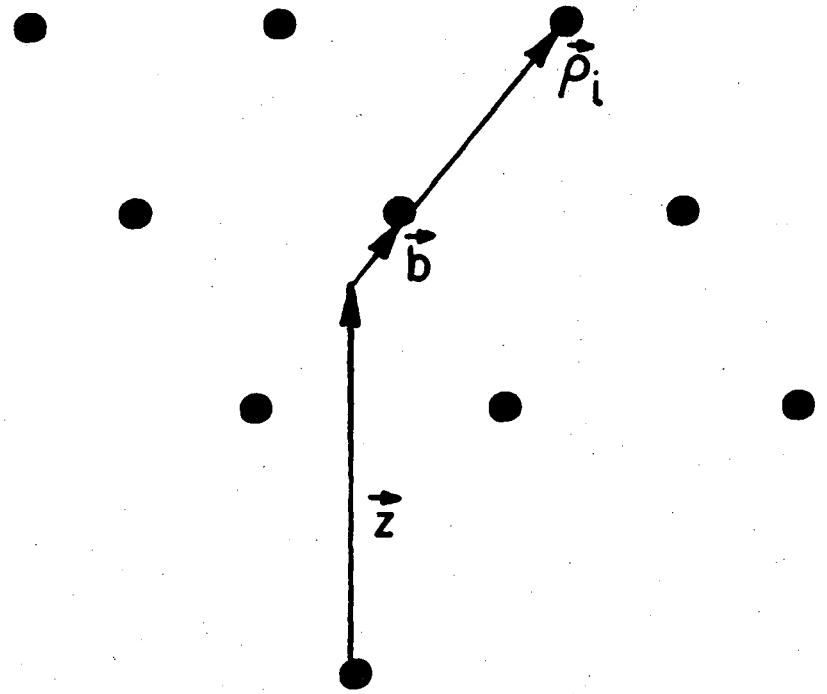

Fig. 1.

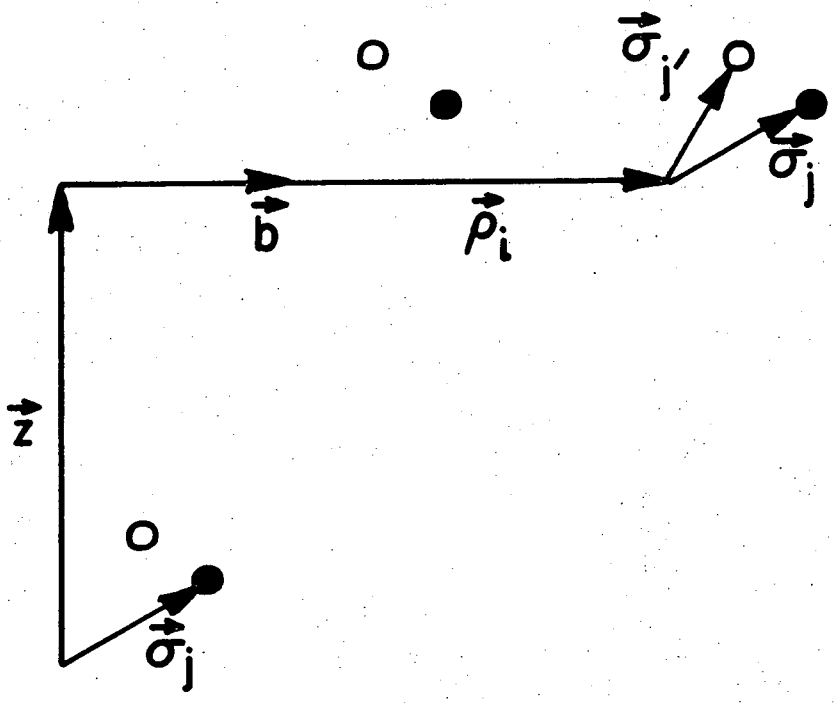

XBL 748-7074

Fig. 2.

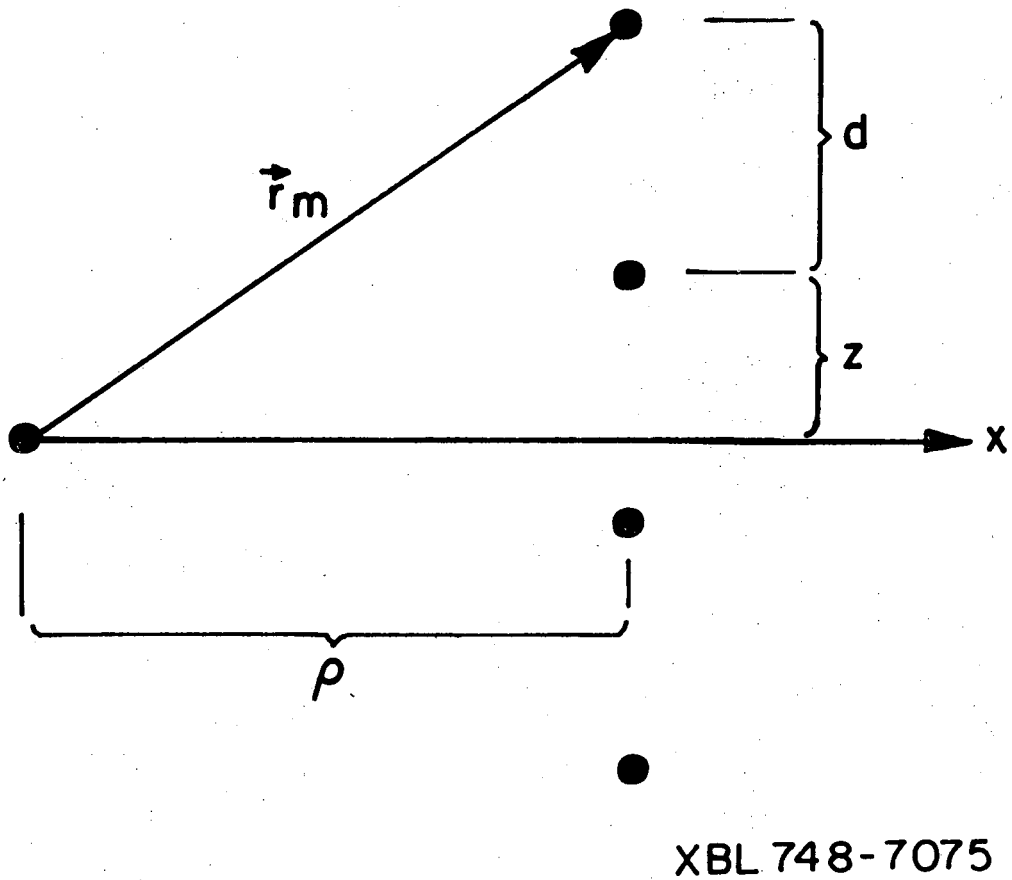

Fig. 3.

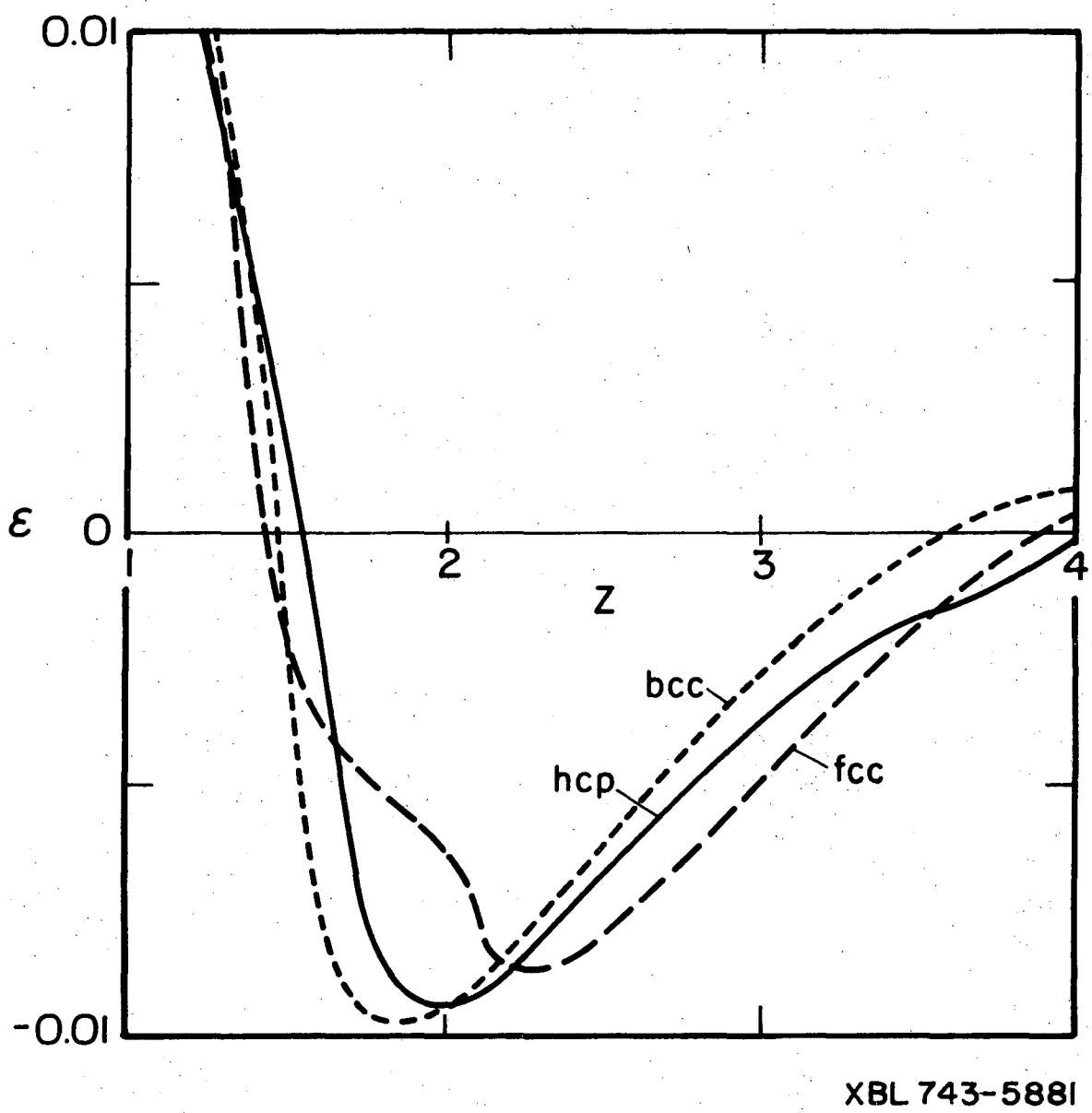

Fig. 4.

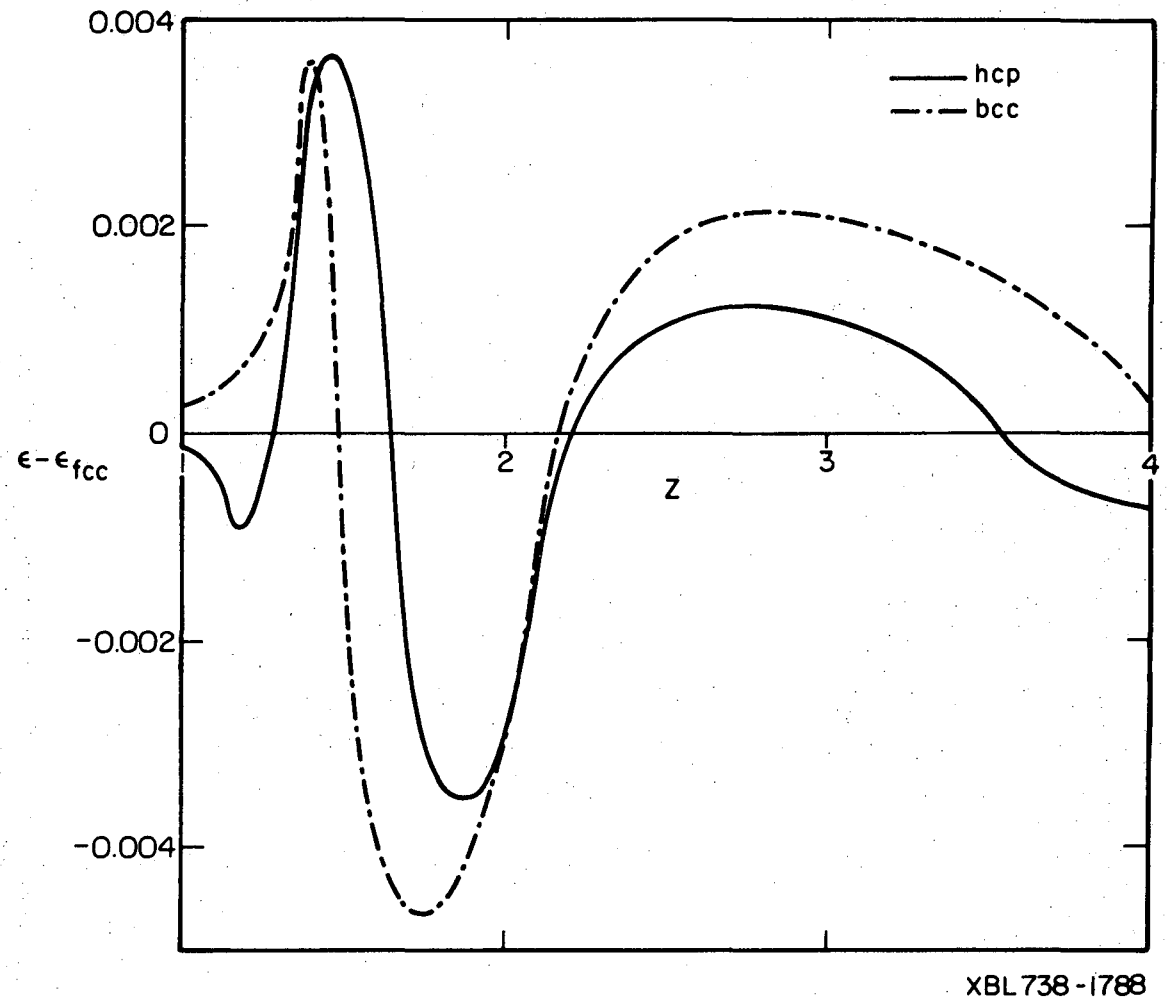
0.004
0.002
0
-0.002
-0.004
$\epsilon - \epsilon_{fcc}$
2
3
4
Z
hcp
bcc
XBL738-1788

Fig. 5.

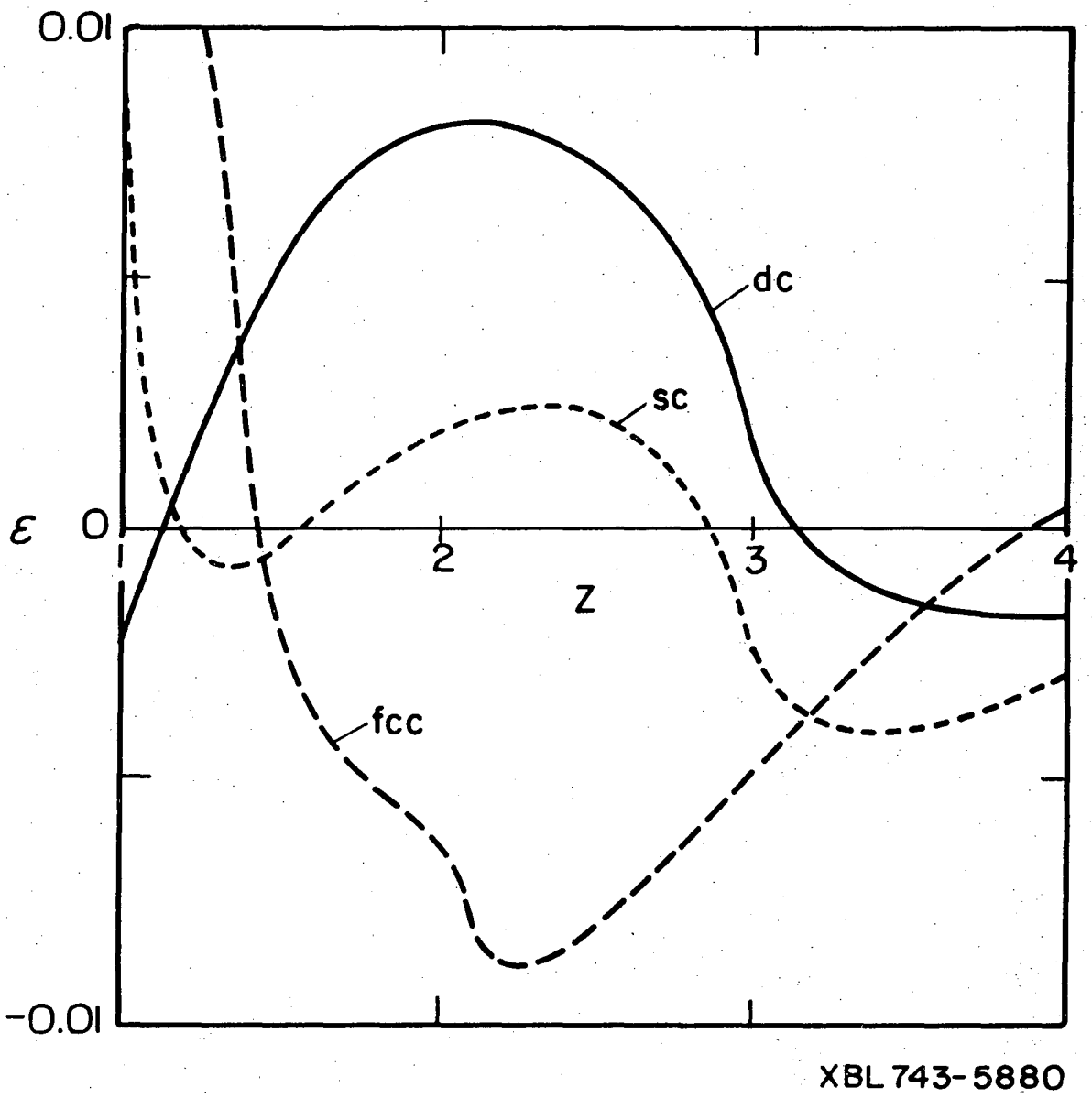

Fig. 6.

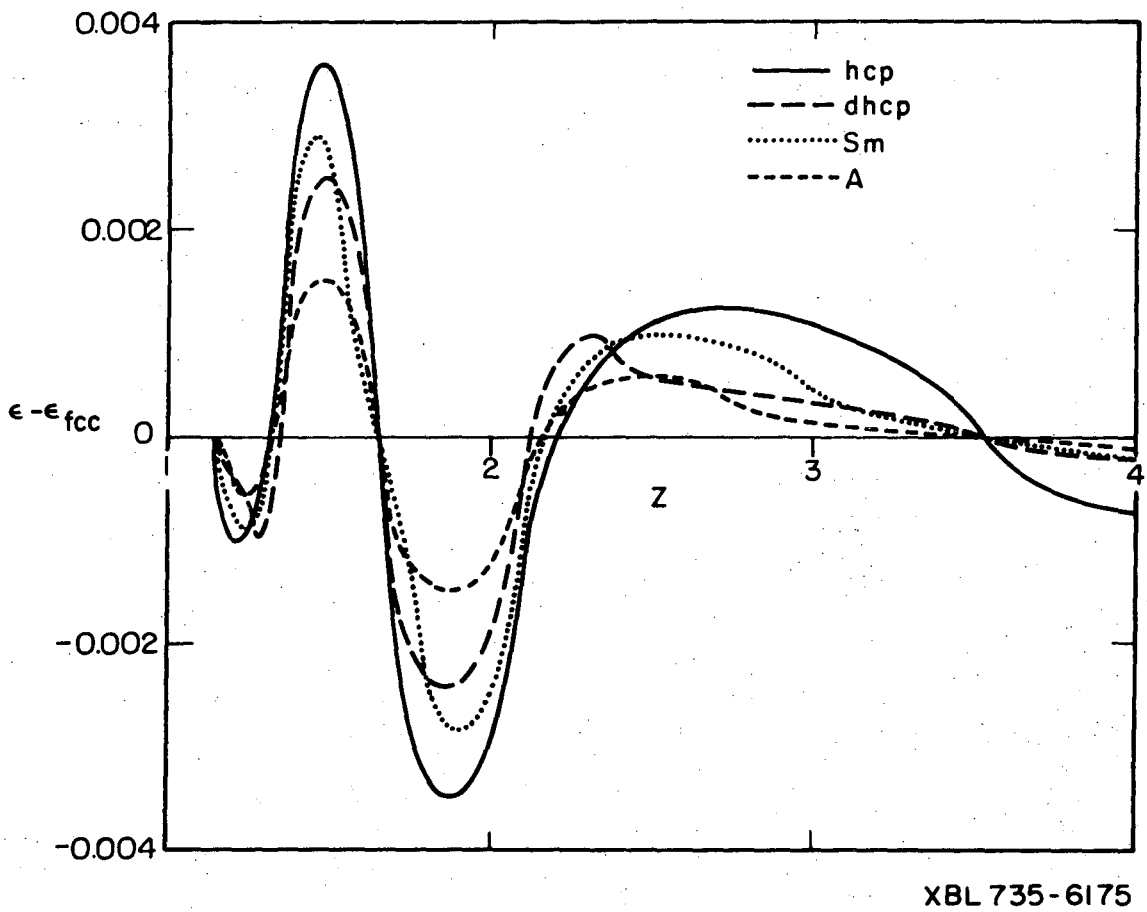
0.004
0.002
0
-0.002
-0.004
$\epsilon - \epsilon_{fcc}$
2
3
4
Z
hcp
dhcp
Sm
A
XBL 735-6175

Fig. 7.

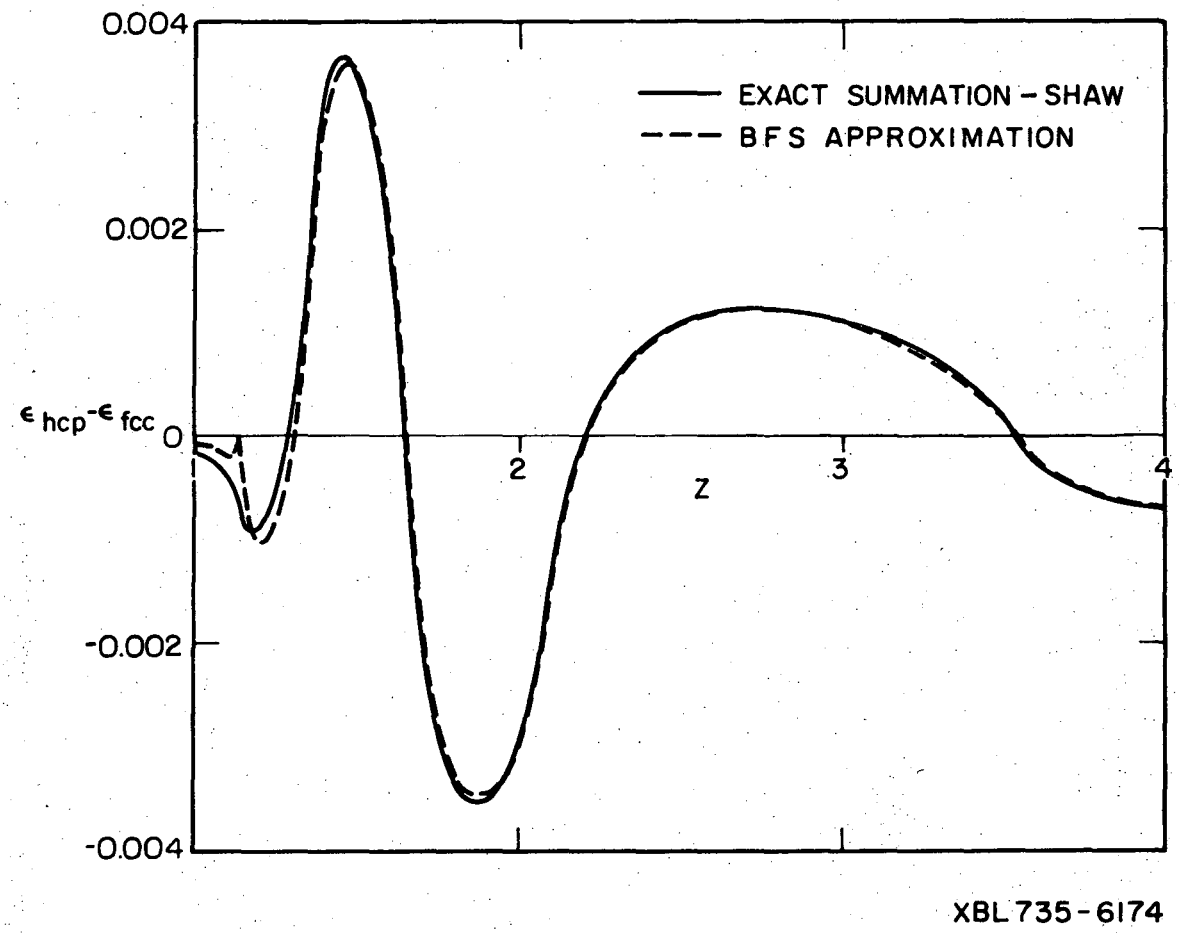
0.004
0.002
0
-0.002
-0.004
$\epsilon_{hcp}-\epsilon_{fcc}$
2
3
4
Z
EXACT SUMMATION - SHAW
BFS APPROXIMATION
XBL 735-6174

Fig. 8.

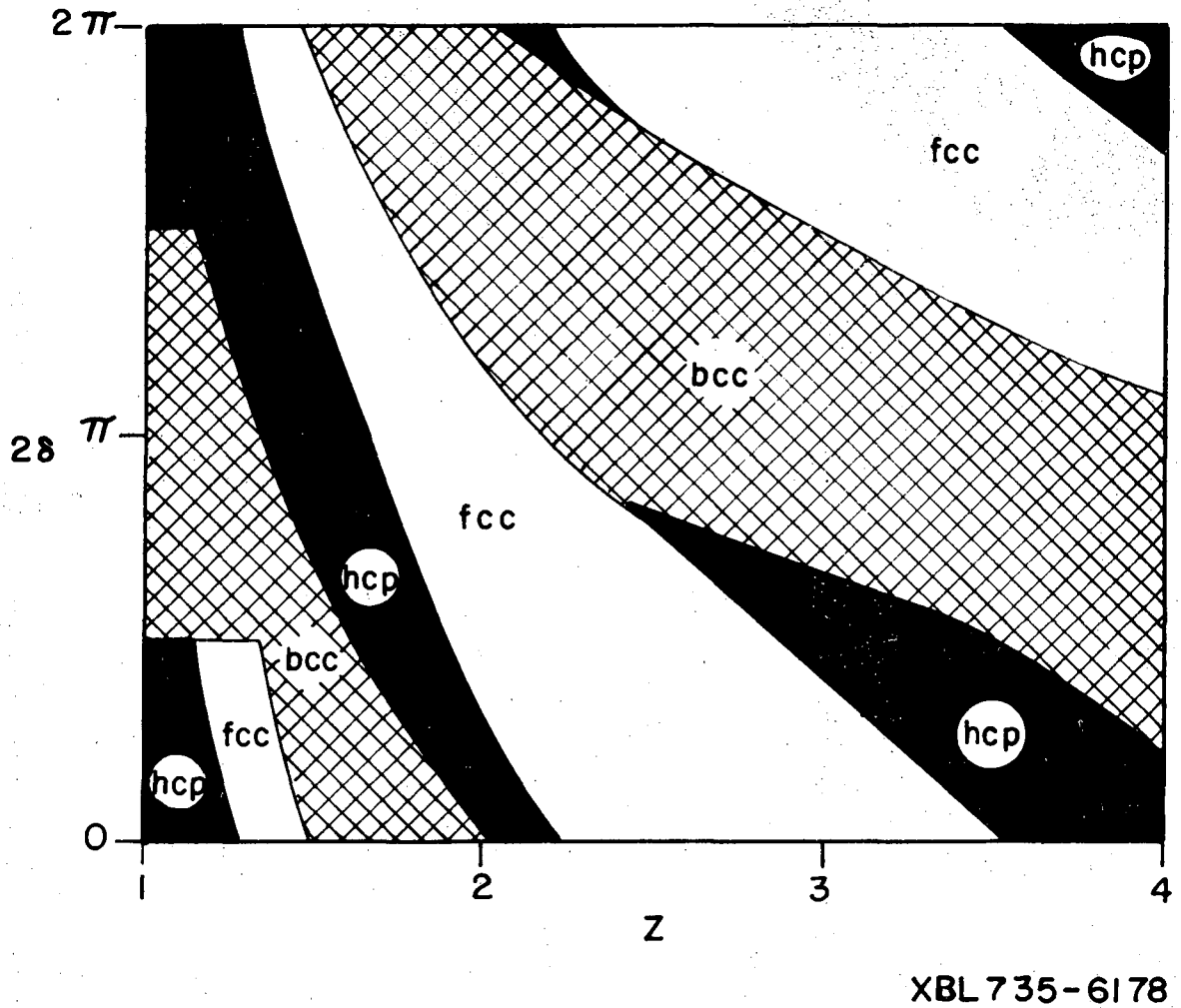

Fig. 9.

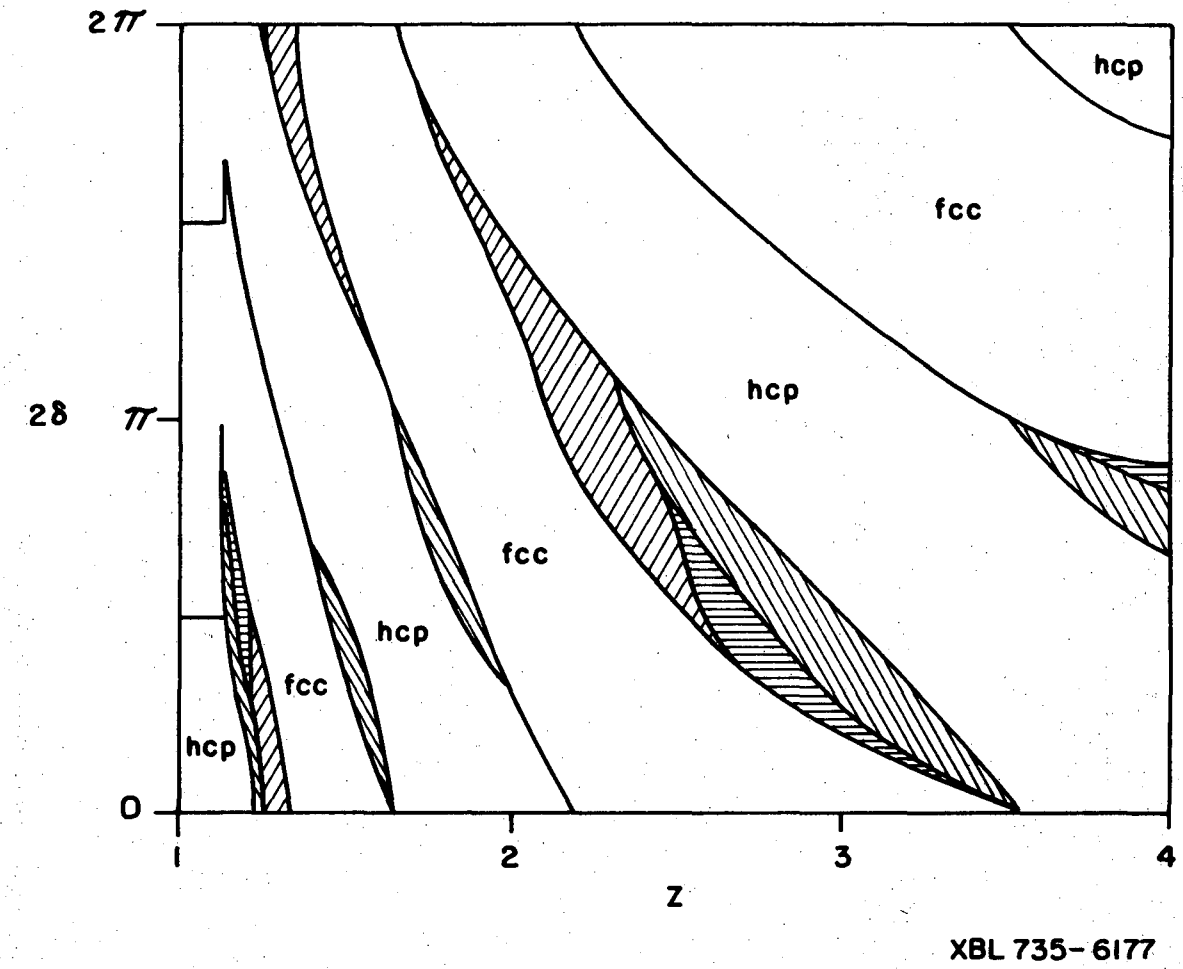

Fig. 10.

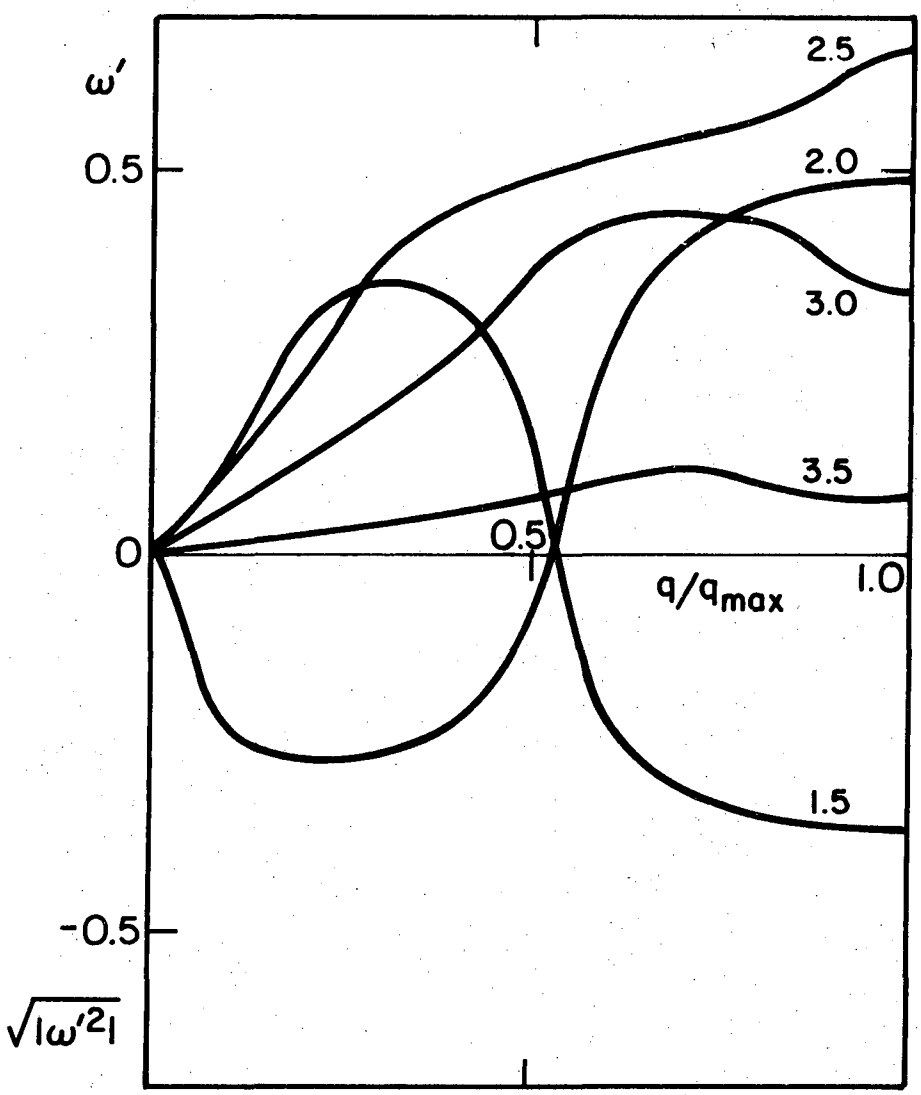

Fig. 11.

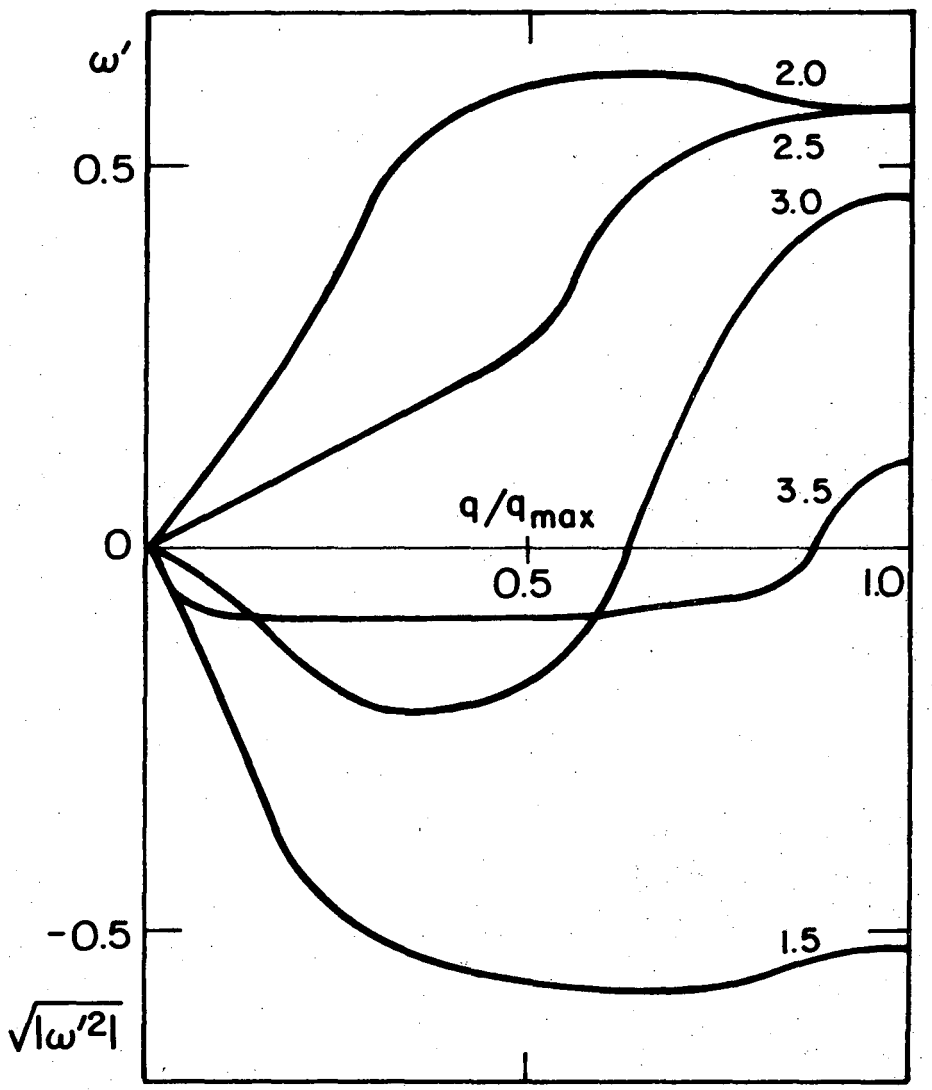

Fig. 12.

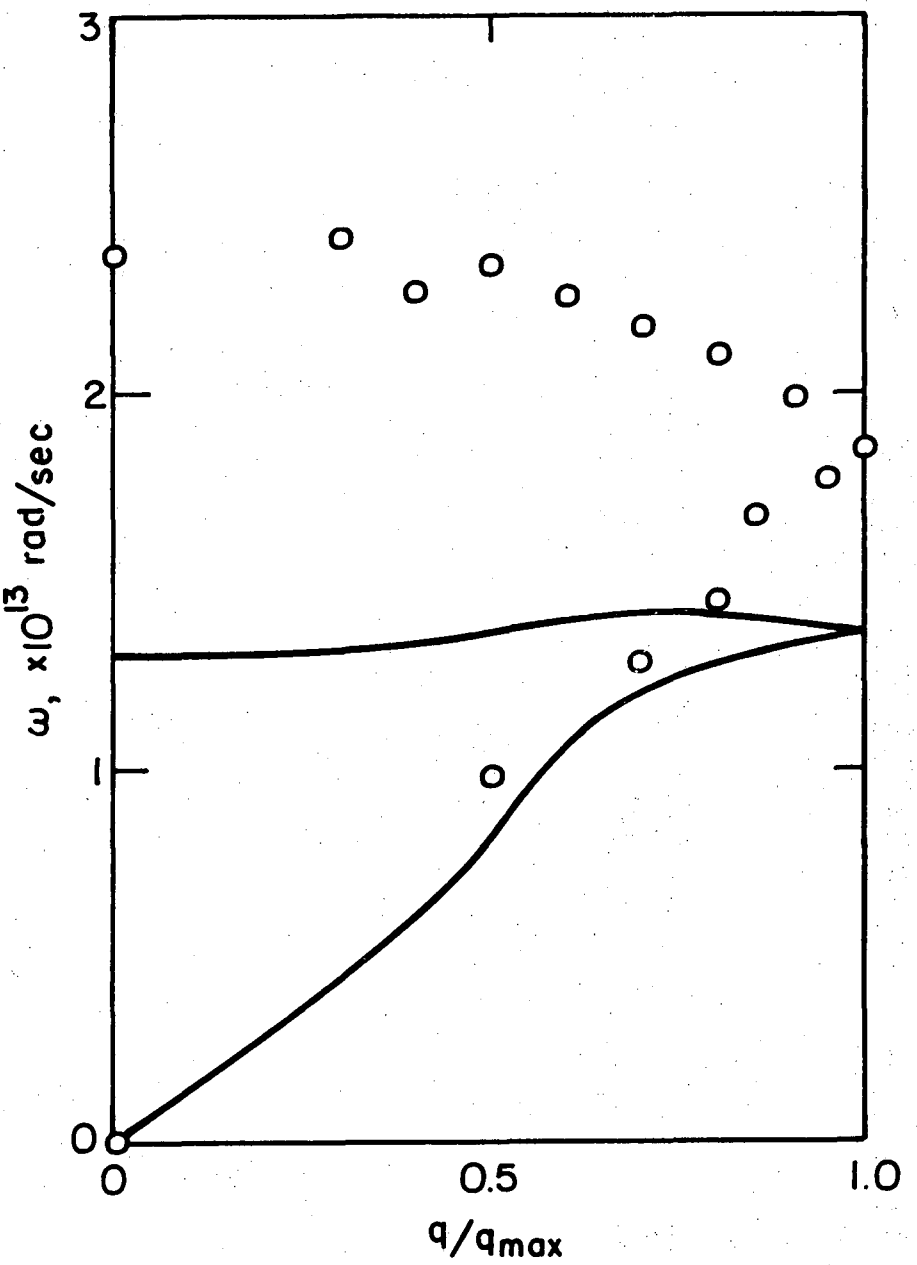

Fig. 13.

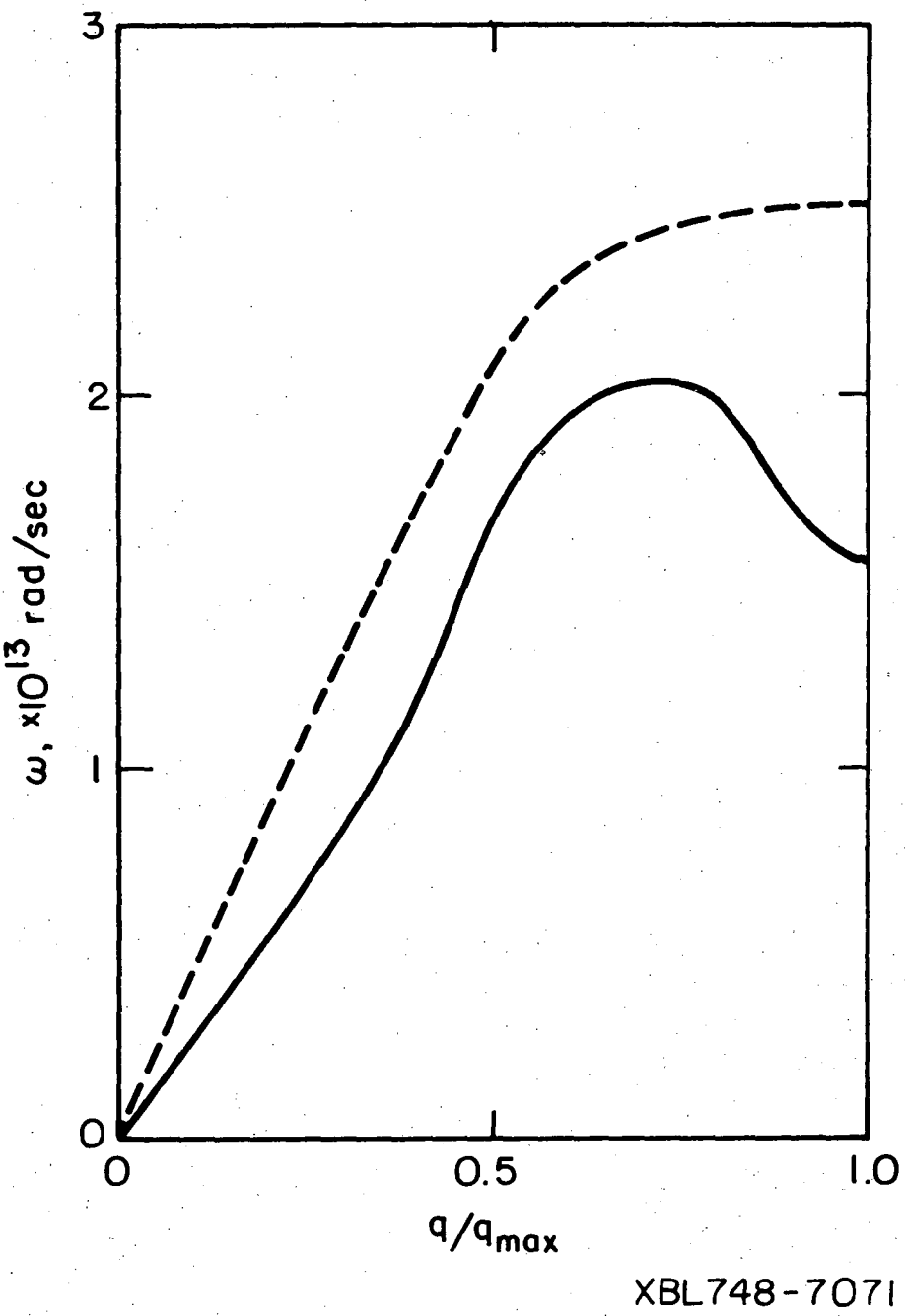

Fig. 14.

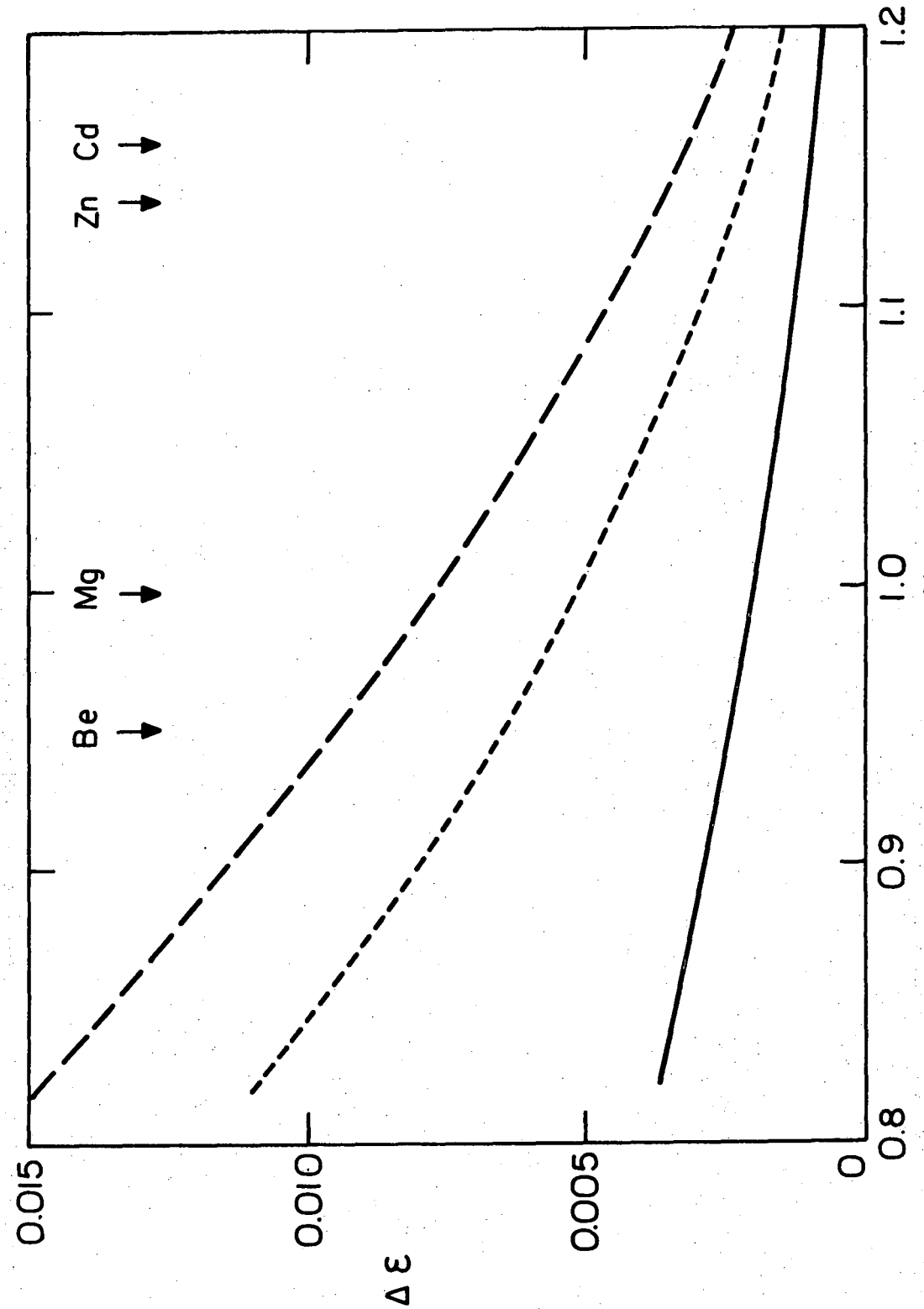

XBL748-7067

Fig. 15.

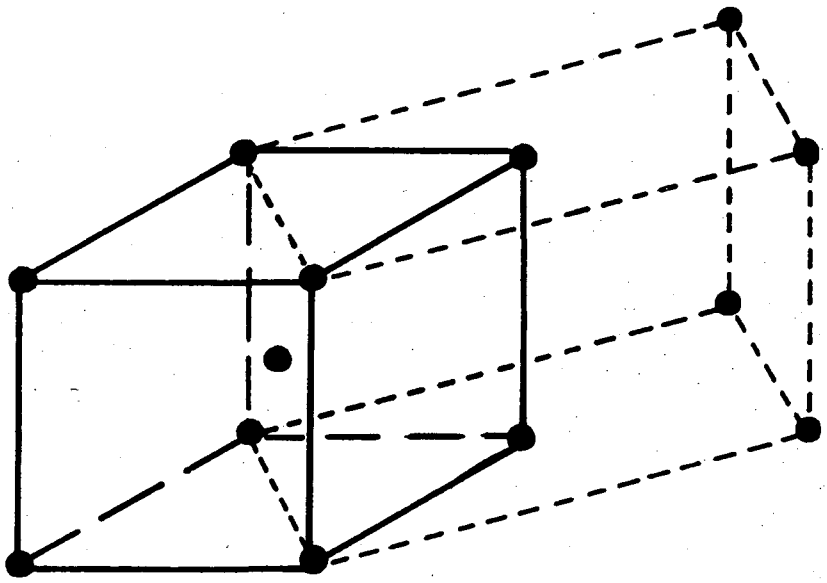

XBL743-5874

Fig. 16.

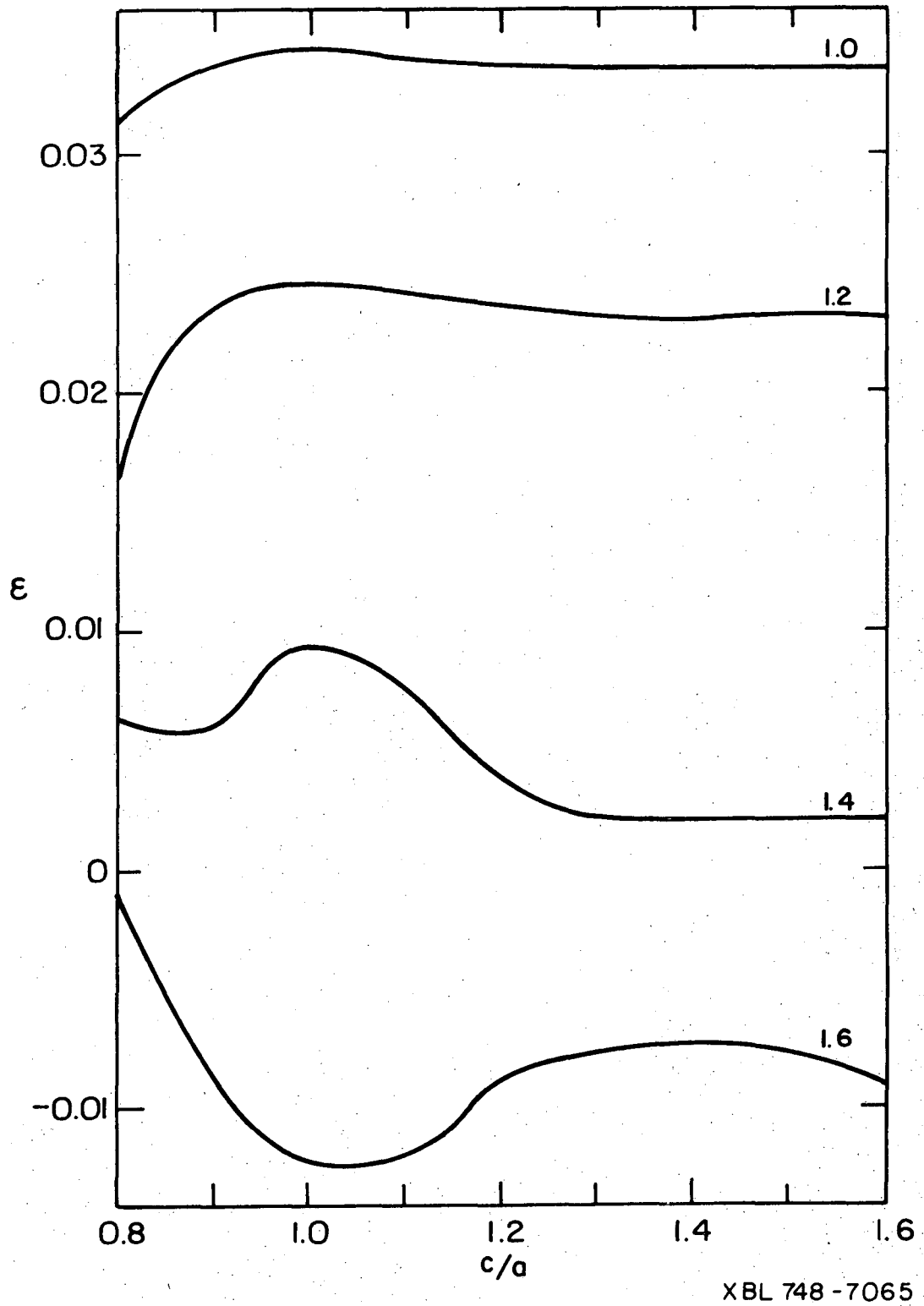

Fig. 17(a).

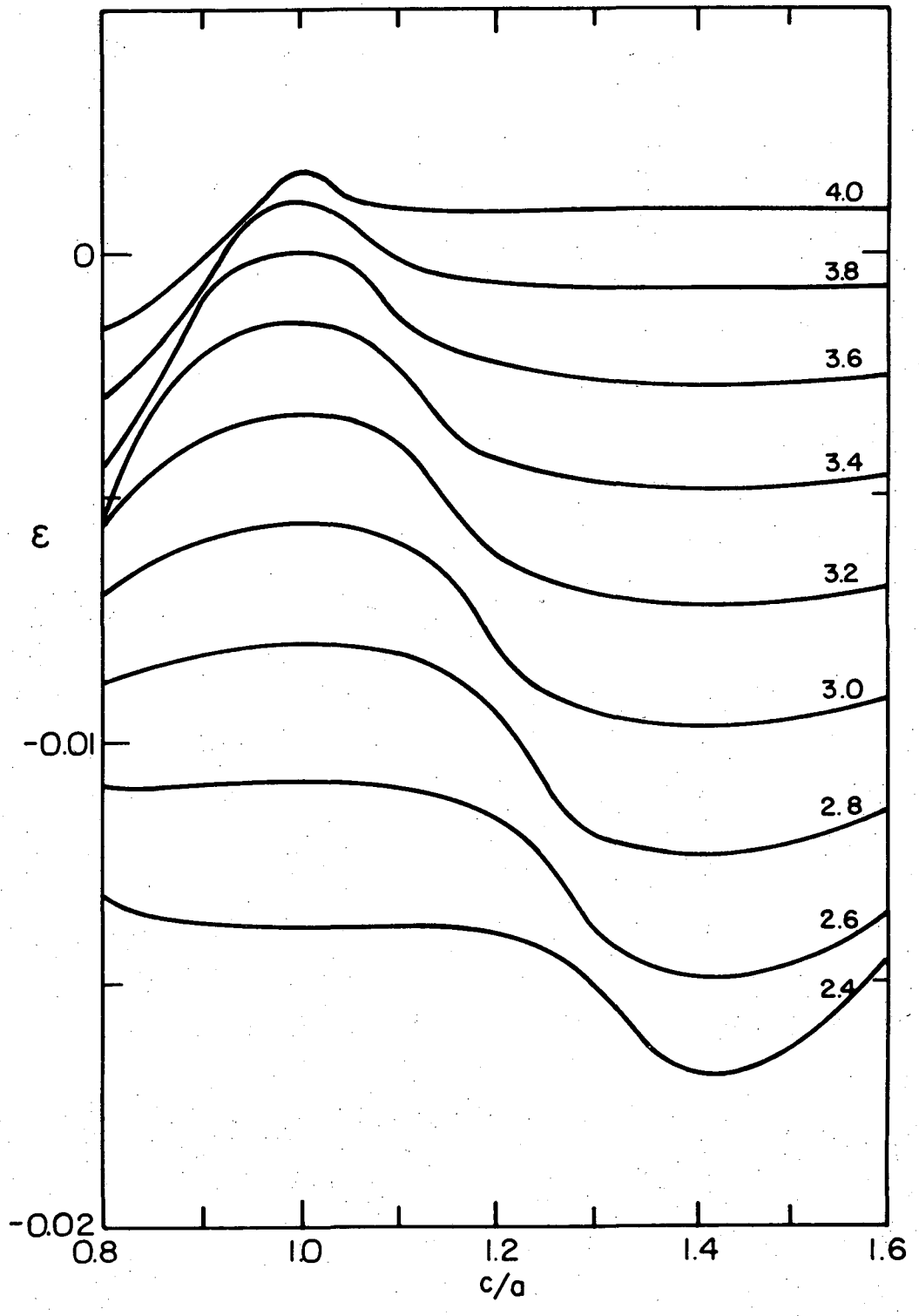

Fig. 17(b).

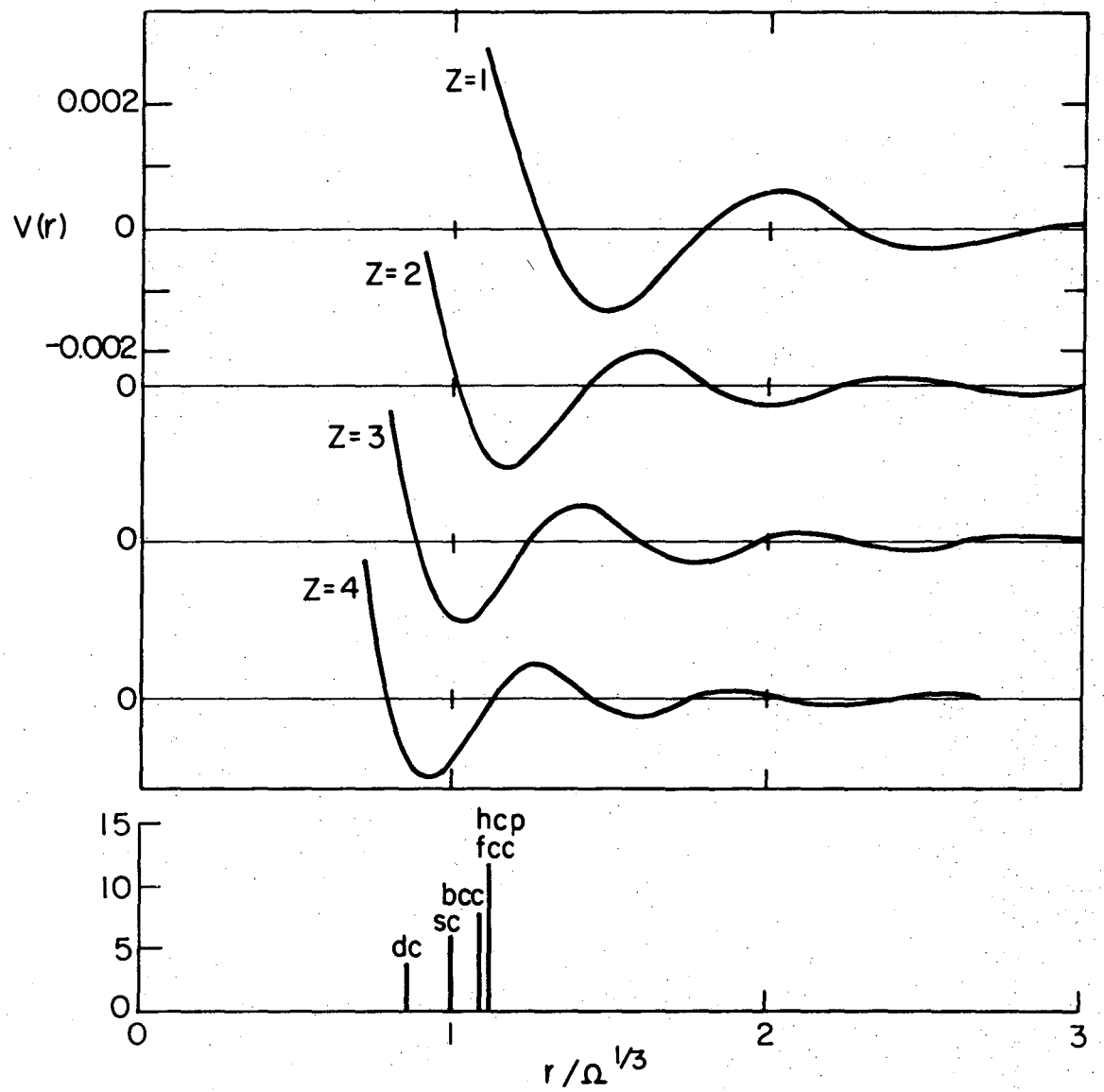
0.002
V(r)
0
-0.002
0
Z=1
Z=2
Z=3
Z=4
0
0
0
15
10
5
0
dc
sc
bcc
fcc
hcp
0
1
2
3
r/Ω 1/3
XBL743-5882

Fig. 18.

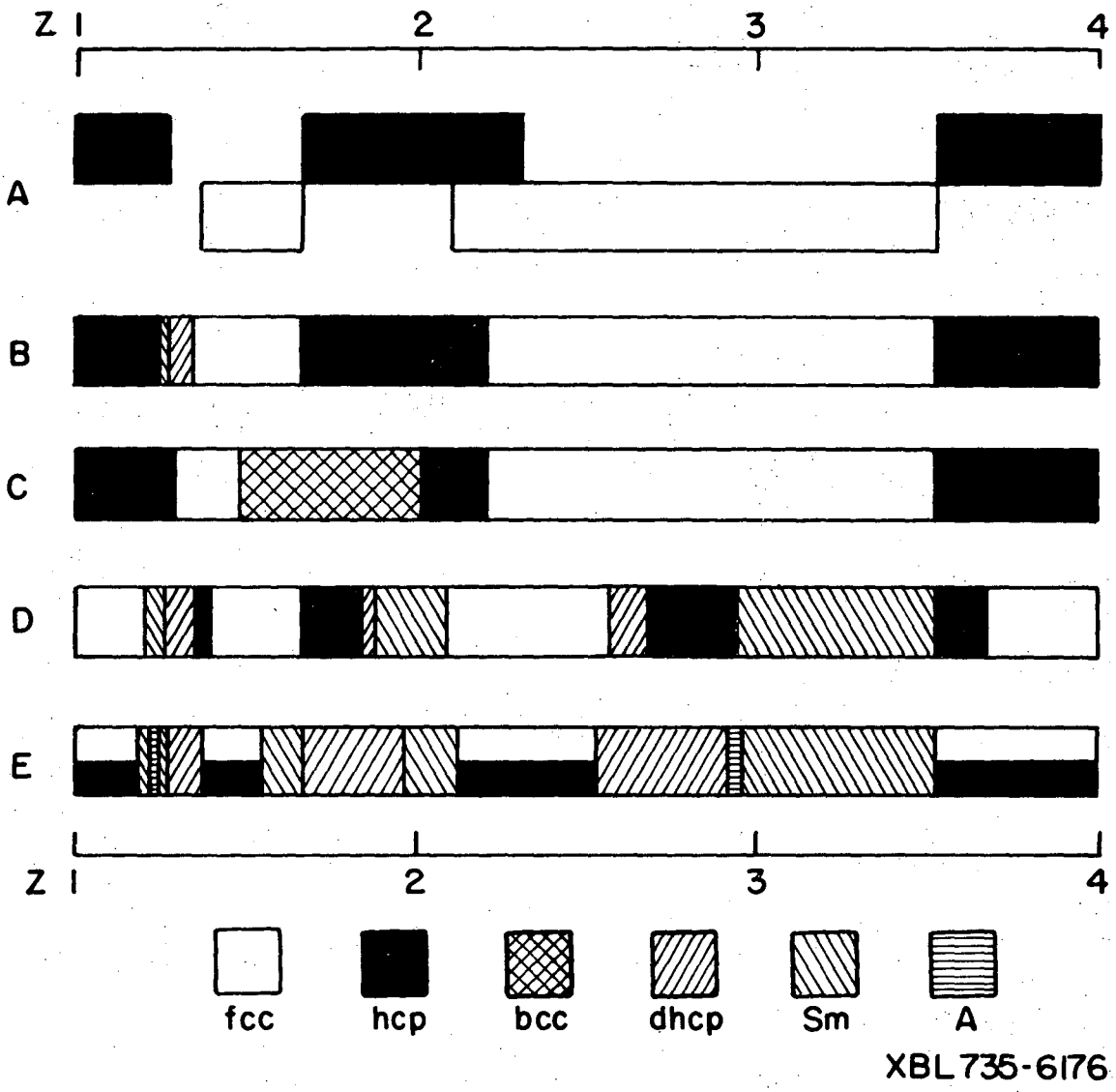

Fig. 19.

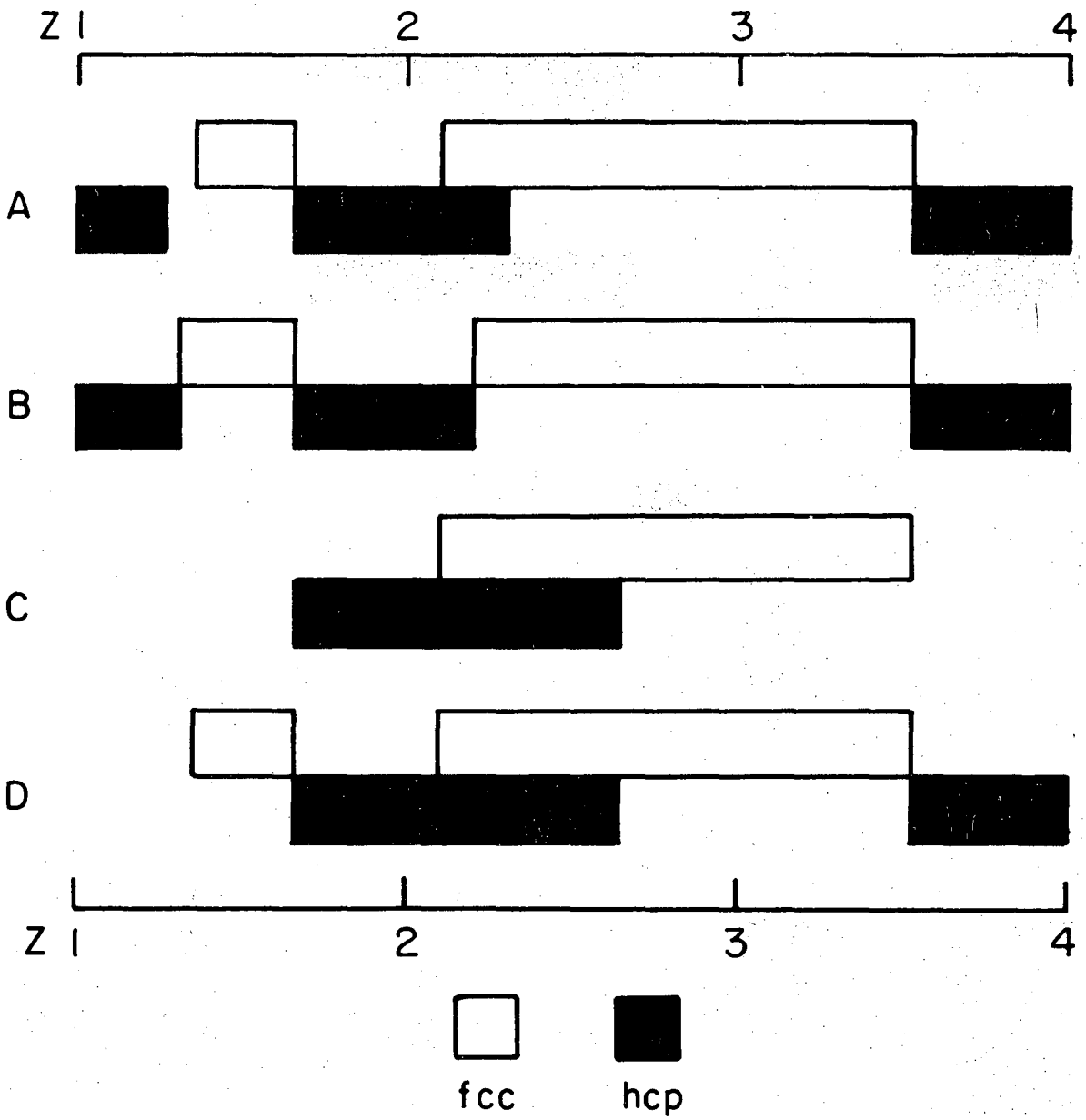

Fig. 20.

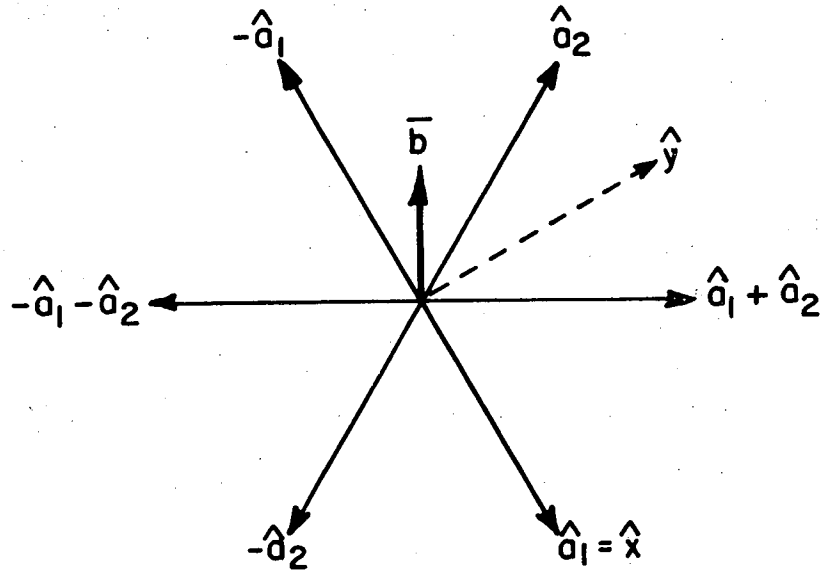

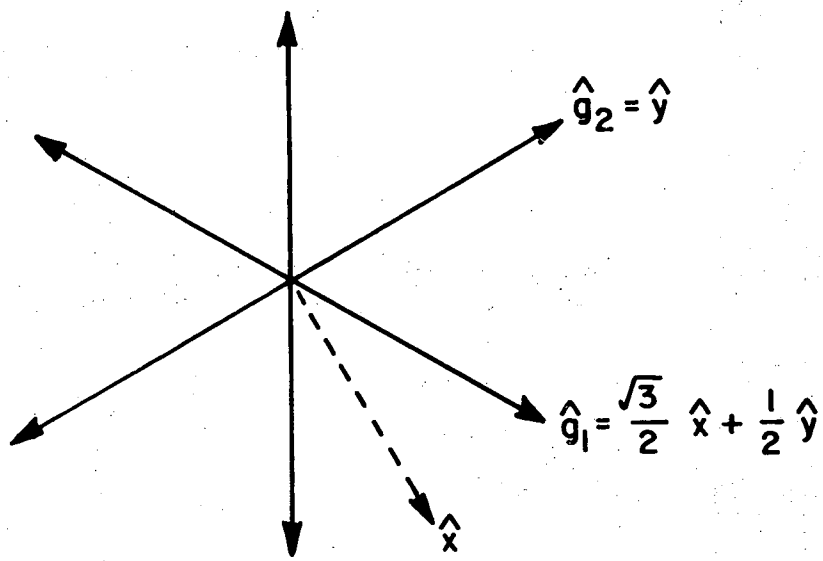

XBL 748-7076

Fig. 21.

TECHNICAL INFORMATION DIVISION
LAWRENCE BERKELEY LABORATORY
UNIVERSITY OF CALIFORNIA
BERKELEY, CALIFORNIA 94720